

Institutionen för systemteknik
Department of Electrical Engineering

Examensarbete

**Model Predictive Control for Series-Parallel Plug-In
Hybrid Electrical Vehicle**

Examensarbete utfört i Fordonssystem
vid Tekniska högskolan i Linköping
av

Jimmy Engman

LiTH-ISY-EX--11/4444--SE

Linköping 2011



Linköpings universitet
TEKNISKA HÖGSKOLAN

Model Predictive Control for Series-Parallel Plug-In Hybrid Electrical Vehicle

Examensarbete utfört i Fordonssystem
vid Tekniska högskolan i Linköping
av

Jimmy Engman

LiTH-ISY-EX--11/4444--SE

Handledare: **Martin Sivertsson**
isy, Linköping University
Christofer Sundström
isy, Linköping University
Ph.D Hongchao Zhang
Infineon Automotive Joint Lab, Tianjin University

Examinator: **Associate Professor Lars Eriksson**
isy, Linköping University

Linköping, 15 June, 2011

	Avdelning, Institution Division, Department Division of Automatic Control Department of Electrical Engineering Linköpings universitet SE-581 83 Linköping, Sweden		Datum Date 2011-06-15
	Språk Language <input type="checkbox"/> Svenska/Swedish <input checked="" type="checkbox"/> Engelska/English <input type="checkbox"/> _____	Rapporttyp Report category <input type="checkbox"/> Licentiatavhandling <input checked="" type="checkbox"/> Examensarbete <input type="checkbox"/> C-uppsats <input type="checkbox"/> D-uppsats <input type="checkbox"/> Övrig rapport <input type="checkbox"/> _____	ISBN _____ ISRN LiTH-ISY-EX--11/4444--SE Serietitel och serienummer ISSN Title of series, numbering _____
URL för elektronisk version http://www.control.isy.liu.se http://www.ep.liu.se			
Titel Title Modellbaserad prediktionsreglering för seriell-parallell plugin hybridfordon Model Predictive Control for Series-Parallel Plug-In Hybrid Electrical Vehicle			
Författare Jimmy Engman Author			
Sammanfattning Abstract <p>The automotive industry is required to deal with increasingly stringent legislation for greenhouse gases. Hybrid Electric Vehicles, HEV, are gaining acceptance as the future path of lower emissions and fuel consumption. The increased complexity of multiple prime movers demand more advanced control systems, where future driving conditions also becomes interesting. For a plug-in Hybrid Electric Vehicle, PIHEV, it is important to utilize the comparatively inexpensive electric energy before the driving cycle is complete, this for minimize the cost of the driving cycle, since the battery in a PIHEV can be charged from the grid. A strategy with length information of the driving cycle from a global positioning system, GPS, could reduce the cost of driving. This by starting to blend the electric energy with fuel earlier, a strategy called blended driving accomplish this by distribute the electric energy, that is charged externally, with fuel over the driving cycle, and also ensure that the battery's minimum level reaches before the driving cycle is finished. A strategy called Charge Depleting Charge Sustaining, CDCS, does not need length information. This strategy first depletes the battery to a minimum State of Charge, SOC, and after this engages the engine to maintain the SOC at this level. In this thesis, a variable SOC reference is developed, which is dependent on knowledge about the cycle's length and the current length the vehicle has driven in the cycle. With assistance of a variable SOC reference, is a blended strategy realized. This is used to minimize the cost of a driving cycle. A comparison between the blended strategy and the CDCS strategy was done, where the CDCS strategy uses a fixed SOC reference. During simulation is the usage of fuel minimized; and the blended strategy decreases the cost of the driving missions compared to the CDCS strategy. To solve the energy management problem is a model predictive control used. The designed control system follows the driving cycles, is charge sustaining and solves the energy management problem during simulation. The system also handles moderate model errors.</p>			
Nyckelord Keywords MPC, series-parallel HEV, Hildreths procedure, Quadratic Programming, plug-in HEV			

Abstract

The automotive industry is required to deal with increasingly stringent legislation for greenhouse gases. Hybrid Electric Vehicles, HEV, are gaining acceptance as the future path of lower emissions and fuel consumption. The increased complexity of multiple prime movers demand more advanced control systems, where future driving conditions also becomes interesting. For a plug-in Hybrid Electric Vehicle, PIHEV, it is important to utilize the comparatively inexpensive electric energy before the driving cycle is complete, this for minimize the cost of the driving cycle, since the battery in a PIHEV can be charged from the grid. A strategy with length information of the driving cycle from a global positioning system, GPS, could reduce the cost of driving. This by starting to blend the electric energy with fuel earlier, a strategy called blended driving accomplish this by distribute the electric energy, that is charged externally, with fuel over the driving cycle, and also ensure that the battery's minimum level reaches before the driving cycle is finished. A strategy called Charge Depleting Charge Sustaining, CDCS, does not need length information. This strategy first depletes the battery to a minimum State of Charge, SOC, and after this engages the engine to maintain the SOC at this level. In this thesis, a variable SOC reference is developed, which is dependent on knowledge about the cycle's length and the current length the vehicle has driven in the cycle. With assistance of a variable SOC reference, is a blended strategy realized. This is used to minimize the cost of a driving cycle. A comparison between the blended strategy and the CDCS strategy was done, where the CDCS strategy uses a fixed SOC reference. During simulation is the usage of fuel minimized; and the blended strategy decreases the cost of the driving missions compared to the CDCS strategy. To solve the energy management problem is a model predictive control used. The designed control system follows the driving cycles, is charge sustaining and solves the energy management problem during simulation. The system also handles moderate model errors.

Sammanfattning

Fordonsindustrin måste hantera allt strängare lagkrav mot utsläpp av emissioner och växthusgaser. Hybridfordon har börjat betraktas som den framtida vägen för att ytterligare minska utsläpp och användning av fossila bränslen. Den ökade komplexiteten från flera olika motorer kräver mera avancerade styrsystem. Begränsningar från motorernas energikällor gör att framtida förhållanden är viktiga att estimeras. För plug-in hybridfordon, PIHEV, är det viktigt att använda den

jämförelsevis billiga elektriska energin innan fordonet har nått fram till slutdestinationen. Batteriets nuvarande energimängd mäts i dess State of Charge, SOC. Genom att utnyttja information om hur långt det är till slutdestinationen från ett Global Positioning System, GPS, blandar styrsystemet den elektriska energin med bränsle från början, detta kallas för blandad körning. En strategi som inte har tillgång till hur långt fordonet ska köras kallas Charge Depleting Charge Sustaining, CDCS. Denna strategi använder först energin från batteriet, för att sedan börja använda förbränningsmotorn när SOC:s miniminivå har nåtts. Strategin att använda GPS informationen är jämförd med en strategi som inte har tillgång till information om körcykelns längd. Blandad körning använder en variabel SOC referens, till skillnad från CDCS strategin som använder sig av en konstant referens på SOC:s miniminivå. Den variabla SOC referensen beror på hur långt fordonet har kört av den totala körsträckan, med hjälp av denna realiseras en blandad körning. Från simuleringarna visade det sig att blandad körning gav minskad kostnad för de simulerade körcyklerna jämfört med en CDCS strategi. En modellbaserad prediktionsreglering används för att lösa energifördelningsproblemet. Styrsystemet följer körcykler och löser energifördelningsproblemet för de olika drivkällorna under simuleringarna. Styrsystemet hanterar även måttliga modellfel.

Acknowledgments

I would first of all thank Professor Lars Eriksson, Linköping University, and Professor Hui Xie, Tianjin University, that made it possible for me to write my thesis in China with such an interesting topic. Martin Sivertsson for valuable inputs and patience with completing the report. Christofer Sundström helped me in the beginning of my thesis and I also would like to thank him.

In Tianjin University I would thank all the people in my lab that made my visit in Tianjin very pleasant, special thanks to Doctor Hong Chao Zhang for valuable thoughts and comments.

I would also thank my family for all the support, my dad for valuable thoughts about practical matters about different components, and particular my girlfriend that with persistent support and great understanding helped me.

Contents

1	Introduction	1
1.1	Background	1
1.2	Outline	2
2	Related Research	3
2.1	Dynamic Programming	4
2.1.1	Deterministic Dynamic Programming	4
2.1.2	Stochastic Dynamic Programming	4
2.2	ECMS and A-ECMS	5
2.3	MPC	5
2.4	Blended Vs. CDCS	6
2.5	Ideas for this thesis	7
3	Problem formulation	9
3.1	Supervisory Control System	9
3.2	Utilization of GPS	10
3.3	Drive cycles and driver	10
4	Hybrid Electric Vehicles	13
4.1	Series Hybrid Electric Vehicles	13
4.2	Parallel Hybrid Electric Vehicles	14
4.3	Series-parallel Hybrid Electric Vehicles	15
4.4	Plug-In Hybrid Electric Vehicles	15
5	System Modeling	17
5.1	Overview	17
5.2	Internal combustion engine	17
5.3	Motor and Generator	19
5.4	Battery	19
5.5	Drive train	20
5.5.1	Planetary gear set	21
5.5.2	Torque Coupler and final drive	22
5.5.3	Longitudinal vehicle model	24
5.5.4	Dynamic Model	25
5.6	Driver	25

6	Supervisory Control System	27
6.1	The plant model	27
6.2	Model Predictive Control	28
6.2.1	Linearization	28
6.2.2	Discretization	28
6.2.3	Augmented model	29
6.2.4	Quadratic Programming	30
6.2.5	Optimization - Active Set	32
6.2.6	Optimization - Hildreth's procedure	33
6.3	Low level controller	35
7	Results	37
7.1	Step response	37
7.1.1	Acceleration	38
7.1.2	CDCS	40
7.2	Sampling time and control horizon	42
7.3	Robustness	44
7.4	Utilization of GPS	45
7.4.1	Highway, Urban and City driving	46
7.4.2	City driving	46
7.4.3	Highway driving	47
8	Conclusions	51
8.1	Step response	51
8.2	Sampling time and control horizon	52
8.3	Robustness	52
8.4	Utilization of GPS	53
8.5	Future work	53
	Bibliography	55

Chapter 1

Introduction

This master thesis project was carried out at Infineon Automotive Electronics Joint Lab, State Key Lab of Engines, Tianjin University. The objective of the thesis is to design a control strategy, that aims to handle the energy management problem for a series-parallel plug-in hybrid electric vehicle. The controller are assisted with a global positioning system.

1.1 Background

Environmental impact from vehicles has recently been under strong debate, demands from customers and politicians urge the automotive industry to take responsibility for pollutions and greenhouse gases. Sustainable and less energy consuming methods of travel are going to be important for the future automotive manufacturers. A hybridization of an electrical and a conventional vehicle increases possibilities of a higher overall efficiency, compared to a conventional vehicle. The hybrid electric vehicle is called HEV, and the plug-in HEV, PIHEV. The PIHEV can charge the battery from the grid. The extra energy source provides electric energy, which compared with energy from fuel is considered relatively inexpensive and locally lower emissions. To fully utilize the benefits of the PIHEV, the control system is required to:

- Optimize use of cheap energy.
- Optimize drive-train, motor, generator, engine and batteries overall efficiency.
- Minimize the use of fuel.

Conventional gasoline engines have a peak efficiency $\approx 37\%$. In regular driving, most driving is made at part-load, this contributes to a low overall efficiency $\approx 17\%$, see [6]. The electric motor has a higher part-load efficiency, $\approx 90\%$, and also a higher peak efficiency, $\approx 94\%$. Through hybridization, this provides a great potential of improving the overall efficiency of a vehicle.

1.2 Outline

In chapter 2 related research is discussed and the problem formulation is defined in chapter 3. Aspects of using a model predictive control system; as well aspects of utilizing a global positioning system, GPS, are also discussed. The chapter 4 describes the architecture of different hybrid electric vehicle systems. A system model and supervisory control system is designed in chapters 5 and 6, the results and conclusions is presented in chapters 7 and 8, where ideas of future work also is presented.

Chapter 2

Related Research

Control system for HEV's can be divided into two main groups, one is called optimal controller, and the other is rule-based controller. The rule-based controller uses rules that are based on experience and engineering judgement. In this thesis a controller that is based on an optimal control strategy is developed.

The optimal controller is based on finding the optimal control law based on a certain criterion. For HEV's, the control law will depend on the driving cycle. Therefore to find the optimal control for a driving cycle, the entire cycle needs to be known. This is referred to as finding the global optimum. The equation (2.1) describes the cost function that are minimized, and \vec{u} denotes the control variable. The end-time of the driving cycle is denoted t_{end} and the function $f(q)$ is the cost associated with the electric energy usage. The energy level of the battery is described by its state of charge, denoted as $q(\vec{u}(t))$, where one is full and zero is a battery that is completely depleted.

$$J_{cost} = \min_{\vec{u}} \int_0^{t_{end}} \left[\dot{m}_{fuel}(\vec{u}(t)) + f(q(\vec{u}(t))) \right] dt \quad (2.1)$$

The equation requires that information about the future driving mission is available; naturally this causes issues with implementation, due to difficulties of predicting the future driving conditions. The more frequent use of a GPS, can overcome some of these shortcomings. Further it provides the possibility to come closer to the global optimum of the entire driving cycle. By using GPS to predict the future route, future power demands can be estimated and utilized to improve the fuel economy.

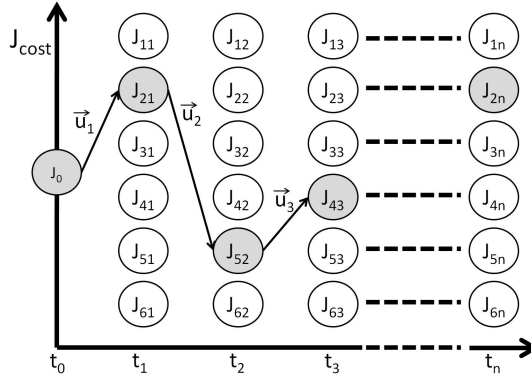


Figure 2.1. All possible costs over a finite time are evaluated to find the sequence that have the smallest total cost. J_n is representing the cost at time step n , depending on what the control variable is selected to, where \bar{u}_n is the control variable at time step n .

2.1 Dynamic Programming

This section only presents the main ideas of Dynamic Programming, called DP. In [6] two types are presented, stochastic and deterministic. A discretization of equation (2.1) is used for both of the strategies. The equation (2.1) is first made discrete where the optimal solution is accurate to grid resolution.

2.1.1 Deterministic Dynamic Programming

Deterministic Dynamic Programming, called DDP, assumes that the disturbance is known in advance. Usage of this algorithm requires that the whole driving cycle is known, and all conditions for the whole cycle is known. This can then give a solution that is finding the global optimum, with a accuracy to discretization resolution. This method is often used as benchmark to compare other developed controllers because it possibilities of finding the global optimum, [2] and [8]. The constraints are enforced by assigning all violations with an infinite cost. In figure 2.1 a multistage decision problem and the optimal sequence of control variables, \bar{u} , is shown. This algorithm is based on that all possible combination is tested to find the minimal cost that an optimal control gives.

2.1.2 Stochastic Dynamic Programming

The Stochastic Dynamic Programming, SPD, assumes that the disturbance is a Markov process, i.e. the probability distribution of the disturbance is not depending on the previous sample. For SDP the probability function for the stochastic variables is required to be known, this variable could be the required torque or power that is needed to follow the driver's demand, velocity or acceleration. This requires information about the future driving conditions. In [7] SDP is used to

investigate what kind of information that is important. The topography showed to be most important, and for vehicles with higher hybridization, the position in the driving cycle is more important than for a vehicle with lower degree of hybridization.

2.2 ECMS and A-ECMS

Equivalent consumption minimization strategy, ECMS, is based on that a cost function consisting of fuel and the fuel equivalent of battery energy is minimized. The weighting variable, σ , is used to compare energy from fuel with energy from battery. The algorithm is using a cost function similar to equation (2.2).

$$J_{cost} = P_e(\vec{u}(t)) + \sigma P_{batt}(\vec{u}(t)) \quad (2.2)$$

In [2] and [8] a developed ECMS controller where using adaption of the weighting factor to maintain charge sustenance for the battery. The adaption uses a variable weighting factor that are between a factor that is favoring charging the battery and a factor that is favoring discharging the battery. This is called adaptive equivalent consumption minimization strategy, A-ECMS, and solved the problem when an ECMS strategy is not charge sustaining.

2.3 MPC

Model predictive control, MPC, can utilize different methods of solving the optimization problem. By using a model of the system, future states can be predicted. In [4] Quadratic Programming, QP, is used for solving the optimization problem.

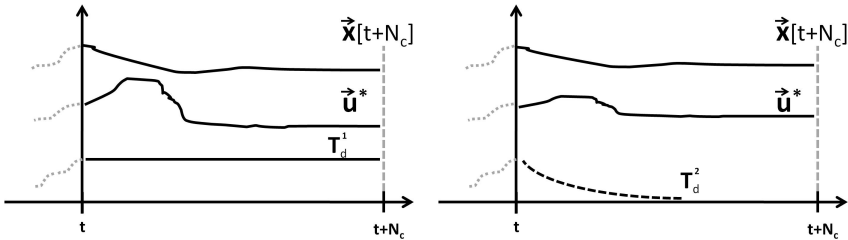


Figure 2.2. The plant model is used to predict future states as a function of the control variable with assumption of future torque's demands from the driver. The control variable is denoted \vec{u} and the states as \vec{x} . The variables T_d^1 and T_d^2 is showing different assumption of future torque's demands.

Discretization and linearization is made to be able to minimize the nonlinear and continuous fuel consumption function. In the article it is assumed that the driver's torque's demands decreases during the prediction time. The figure 2.2 is illustrating two different assumption of the driver's torque demands. T_d^1 assumes that

the driver's demanded torque is constant during the prediction horizon, and T_d^2 assumes that it is decreasing. In this article rules depending on the magnitude of the torque's demands from the driver is used to modeling the driver's torque demands over the prediction horizon. A substantial amount of the ideas in this thesis originates from this article.

DP as optimization algorithm, with model predictive control, is used in [1]. In this article, conversion from a model's time-dependent to route-dependent is presented. A GPS is used to predict future driving conditions; this could lead to improved fuel economy compared to not using any information from a GPS. In the article knowledge of topography is known, and assumption of a constant vehicle speed during the prediction horizon, is used to predict future torque's demands from the driver.

2.4 Blended Vs. CDCS

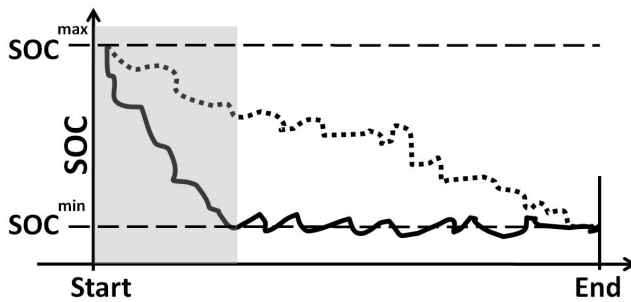


Figure 2.3. Blended driving is the dashed line and the Charge Depleting Charge Sustaining, CDCS, is the solid line. The grey area is representing the All Electric Range, AER.

The relative inexpensive energy from the battery is required to be used as much as possible to minimize the cost to driving the vehicle. The batteries energy level is described by its state of charge, SOC. This can be accomplished with two strategies, both is shown in figure 2.3. The gray area shows the All Electric Range, AER, which is the length that vehicle can drive on exclusively using electric energy. A strategy that is called Charge Depleting Charge Sustaining strategy, called CDCS strategy, uses all the electrical energy until the battery reaches the minimum level of SOC, before it begins to utilize energy from the fuel. The other strategy has knowledge about the mission's length and is using energy from fuel earlier than the CDCS strategy. This strategy is called blended driving and has slower depletion of energy in the battery. In [10] is it shown, that from the start of a driving cycle, blending the use of energy from the battery, with the energy from the fuel, can decrease the total cost of a driving cycle. Blended strategy requires knowledge of

the cycle's length, which can be realized with a GPS. The developed strategy in [10], is using SDP to find the optimal control sequence. Length information of the cycle is modeled as a stochastic variable and the knowledge of the cycle's length resulted in that the SOC depletes slower. It is also shown that a shorter cycle's length than the actual cycle length did not cause a higher cost.

2.5 Ideas for this thesis

In [7] and [1] it is shown that knowledge of position in a driving cycle can decrease the fuel consumption, therefore knowledge of the total length and the current position of the driving cycle is known in this work. In [2], issues of robustness for an ECMS strategy require an adaptive weighting factor to maintain charge sustenances. In [1] the weighting factor is adjusted depending on the torque's demands from the driver. In this thesis a constant weighting factor for all conditions is used, but an adaptive weighting factor would probably give better charge sustenances properties. Due to time limitation, this is not to consider. As in this article, this thesis also use QP as optimization algorithm. According to [10], the blended strategy gives a slower depletion of the SOC, to accomplish this, a variable reference SOC are developed in this thesis. By using information of the cycle's length and current position, the variable reference SOC is linearly decreasing from the initial value to the minimum SOC. This reference is used in the controller that penalizes the deviation from the current SOC and the variable reference SOC.

Chapter 3

Problem formulation

The focus of this master thesis is to develop a supervisory control system that solves the energy management problem and minimize the cost of a drive mission with usage of GPS. The strategy used for control is called model predictive control, MPC. The strategy should be charge sustaining and consider constraints. Charge sustaining is defined as the batteries energy is maintained above a predefined minimum level during the drive cycle. The strategy is evaluated with and without information from a GPS. In this thesis no analysis of the emissions is done, nor is it considered to be minimized in the control system.

3.1 Supervisory Control System

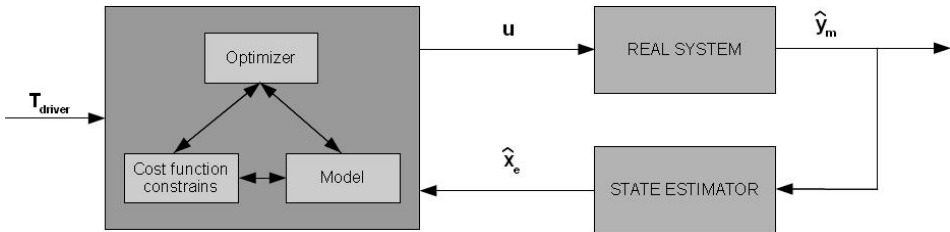


Figure 3.1. Demanded torque from the driver and the estimated states, if one exist, are input signals to the controller.

The concept of a general MPC is illustrated in figure 3.1, the strategy can be divided into four stages:

1. Sampling the estimated or measured states from the system.
2. The optimizer minimizing the cost function with constrains over a time period. The optimization is made with an internal model, known as a plant model.

3. The first optimal control signal is applied on the system until new inputs are available from the state estimator.
4. Return to step 1.

Future input signal from the state estimator and torque demands from the driver are unknown, therefore a plant model is required. The complexity of this model could be reduced to reduce computational efforts. The equation (3.1) describe a discrete cost function over a time window N_c with the weighting factors w_1 and w_2 . The state of charge is denoted as q .

$$J_{cost} = \sum_{k=T_0}^{T_0+N_c} \left(w_1 \left\| \Delta m_{fuel}[k] \right\|^2 + w_2 \left\| q[k] - q^{ref} \right\|^2 \right) \quad (3.1)$$

Issues arising with an MPC controller are; selection of optimization algorithm, sampling time, control horizon and predictive horizon. Note that the predicted horizon can be longer than the horizon where the control output is calculated.

3.2 Utilization of GPS

A Global Positioning System assist the controller with information of the drive mission. In [10] it is shown that blended driving might reduce the cost of the driving if blended driving is encouraged by the controller. In the beginning of the drive cycle the controller needs to restrict electric energy usage, otherwise the motor will use all the available energy from the battery. When the battery then reaches the minimum level, it engages the engine and starts to run in CDCS mode. Consequently there will not be any driving in blended mode, the solution will almost become trivial and no information from the GPS is required.

GPS systems already have functionality of duration and length of the driving mission implemented, this information can then be provided to the controller. The future demands from the driver and information of topography is, in this thesis, considered unknown. The length of the mission can be regarded as reliable. The influence of speed limitations, weather and traffic condition influence the time information, time information is consequently regarded as uncertain.

3.3 Drive cycles and driver

A drive cycle is a standardized velocity profile used to objectively compare vehicles fuel consumption and emission. Here the Federal Test Procedure - U.S standard drive cycle, called FTP-75, the supplement drivecycle, SFTP-US06, and New European Drive Cycle, called NEDC, are used to simulate a driving mission. The figure 3.2 illustrate all the cycles. The SFTP-US06 is used to complement the lack of highway driving in the FTP-75 cycle. Extending the presented cycles is necessary, otherwise the electric range of the studied vehicle cover a significant part of the the drive cycles, for FTP-75 \approx 40% and NEDC \approx 80%. Extensions

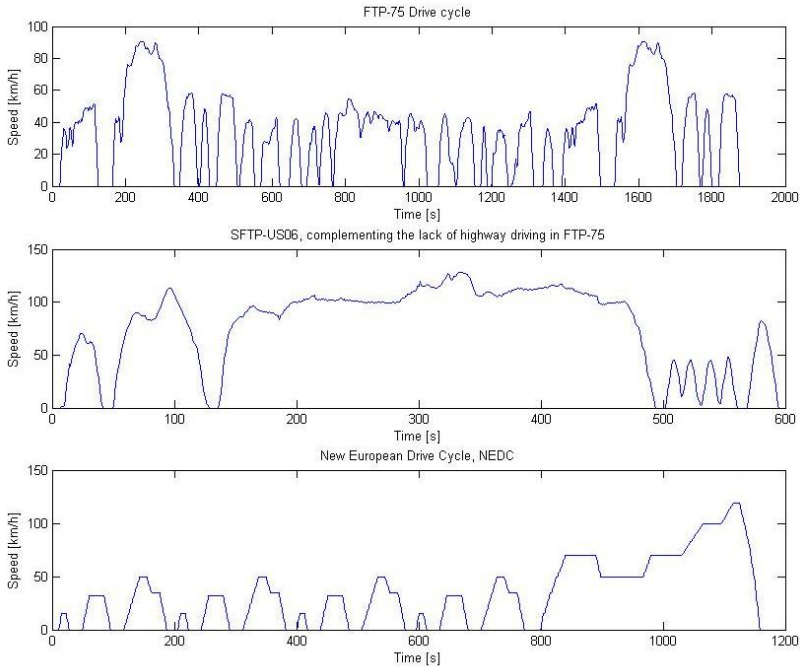


Figure 3.2. The top illustrate the FTP-75 cycle, middle SFTP-US06 and the bottom the NEDC drive cycle.

are made by repeating the cycles in arbitrary order. The extended cycles are addressed in chapter 7. Various extensions will reflect the performance of the controller in different circumstances, consequently those extended drive cycles can provide insight on the controllers robustness and when blended driving is preferred.

Through a feedback signal the velocity profile is translated to a desired torque out from the vehicle. From nonlinearities in the vehicles dynamic equation, large velocity changes can with a linear PI-controller translate the required torque incorrect. In the presented cycles, acceleration and deceleration should not impose any issues, due to the relative slow velocity changes.

Chapter 4

Hybrid Electric Vehicles

The different HEV configurations are briefly presented in this chapter. Since there are several variations of the presented configurations, the chapter aim is only to give the reader a short overview. The text focus on full hybrids, less hybridized vehicles is not considered in this chapter. The main advantages, that do not need to apply for all configurations, are considered as:

1. Possibilities to recuperate kinetic energy.
2. Extra degree of freedom, due to the multiple prime movers, enables part-load to be shifted to more efficient regions.
3. Downsized engine and motors co-operate to fulfill the maximum power demands.
4. Reduce engines idle time, by only engaging the engine when necessary.

The PIHEV's battery can be charged from the grid. For a HEV, the energy is derived from fuel. Amount of energy in the battery is often measured with its state of charge, SOC, which are dimensionless and is one for a full battery and zero for empty battery.

4.1 Series Hybrid Electric Vehicles

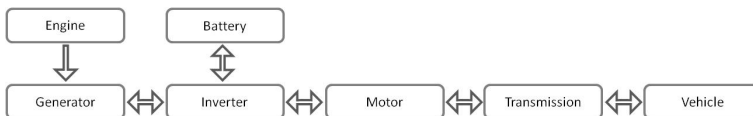


Figure 4.1. The motor in this configuration is also working as an alternator, which enables it to recuperate kinetic energy.

A series HEV utilize the engine to extend the vehicles range, this enables the engine to be designed for average power requirements. Since the engine is decoupled from the drive-train, it can be utilized at a high efficiency region and with low emissions. Minimized idle time is also possible by turning off and on the engine. Series configuration demands that the motor is designed to fulfill maximum power demands. The added weight and multiple energy conversions might lead to lower overall efficiency of the drive train, in particular at highway drive. In general the series architecture has advantages in urban and city driving. Figure 4.1 illustrates the basic power path in a series HEV.

4.2 Parallel Hybrid Electric Vehicles

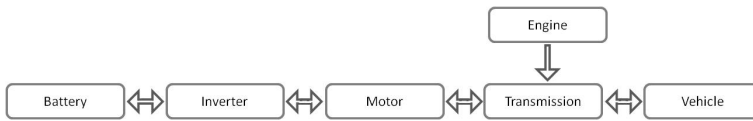


Figure 4.2. The figure is showing a full parallel hybrid architecture, where the engine can provide traction power to the drive train.

Parallel configuration utilizes the engine and motor to co-operate to fulfill high power demands. The parallel configuration in figure 4.2 can only charge the battery when the vehicle is moving.

Clearly this can pose issues, if the energy level in the battery does not permit the motor to be engaged. For instance, SOC level is at minimum level, therefore the engine is required to deliver all the power. If the available power is less than the required it results in that the desired power from the driver is not reached.

This configuration enables possibilities of minimized idle time, presuming that the transmission allows the engine to be disengaged. Main advantage for parallel hybrids is the possibilities of directly engage the engine to provide traction to the vehicle, with no additional losses due to conversion to electricity.

4.3 Series-parallel Hybrid Electric Vehicles

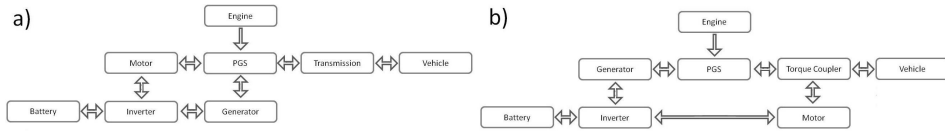


Figure 4.3. a) An configuration that make it possible to drive in electric mode, engine only mode or a combination. b) An similar configuration as in this thesis, where the architecture in this thesis allows the battery to be charged from the grid. The planetary gear set is in the figure called PGS.

In the architecture in the figure 4.3 the generator can also operate as motor, i.e. alternator. The planetary gear set, PGS, along with the generator, realize a Electronically-controlled variable transmission, e-CVT, making it possible to freely control the engines angular speed. Advantages from series and parallel hybrid can with proper design both be utilized with a series-parallel configuration. This is possible since series-parallel HEV can work as series and parallel HEV. Series-parallel is also referred to as split hybrid, dual-mode and combined HEV. Complexity, added weight and increased development cost are the main disadvantages.

4.4 Plug-In Hybrid Electric Vehicles

All presented architecture can be equipped to charge the battery externally. The HEV is then called plug-in hybrid electric vehicle, PIHEV. For these types, it is important to utilize all the energy in the battery, since externally charged energy often is inexpensive compared to the fuel.

Chapter 5

System Modeling

5.1 Overview

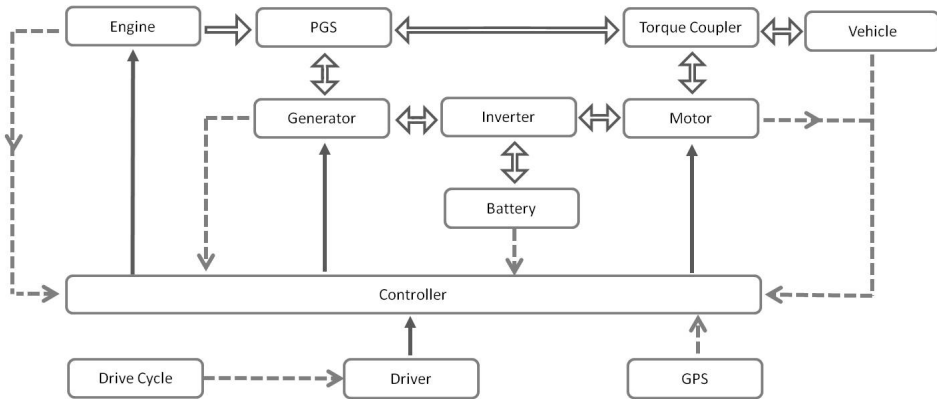


Figure 5.1. Dashed arrow represents data to the controller, solid arrows are power flows and small solid arrows are desired torques.

Figure 5.1 illustrates the interaction between the different subsystems in the HEV system. The components engine, motor and generator are controllable with the torque demands. Signals that are available for the controller are SOC, vehicle velocity, GPS data and angular velocity for engine, motor and generator.

5.2 Internal combustion engine

The model and parameters in this section are from [6], parameters are adjusted to an engine with a volume of $1[dm^3]$ instead of $0.71[dm^3]$. The engine's volume is decided by Tianjin University. An engine with 100% efficiency would produce

a mean effective pressure of p_{mf} from the burning mass. The chemical power is then described by equation (5.1) and (5.2), substitution lead to the relationship in equation (5.3).

$$P_c = p_{mf}V_d \quad (5.1)$$

$$P_c = q_{lhv}\dot{m}_f \quad (5.2)$$

$$p_{mf} = \frac{q_{lhv}\dot{m}_f}{V_d} \quad (5.3)$$

Normalized angular velocity and torque is done with equation (5.4) and (5.5).

$$c_m = \frac{\omega_e S}{\pi} \quad (5.4)$$

$$p_{me} = \frac{T_e \pi N}{V_d} \quad (5.5)$$

The equation (5.6) describe power losses derived from the Otto-cycle, i.e. thermodynamic cycle and mechanical friction losses. This is a general and simplified approach, referred to as Willians line. This is used to estimate the fuel consumption as a function of angular velocity and torque.

$$p_{me} \approx e(c_e)p_{mf} - p_{me0}(c_e) \quad (5.6)$$

A first and second order adaption, as equation (5.7), is made for $p_{me0}(\omega_e)$ and $e(\omega_e)$ respectively. The data is estimated from figures in [6].

$$e(c_e) = e_0 + e_1\omega + e_2\omega^2 \text{ and } p_{me0}(\omega_e) = p_0 + p_1\omega + p_2\omega^2 \quad (5.7)$$

Willians lines equation and parameters are from [6]. By solving equation system (5.6) with (5.3) the fuel consumption is given by (5.8).

$$\dot{m}_f = V_d \frac{p_{me} + p_{me0}(c_m)}{q_{lhv}e(c_m)} \quad (5.8)$$

Notation for engine

S	Bore length of engine [m]
N	Depending on engine, here four stroke $N = 4$
V_d	Engine volume [m ³]
T_e	Engine torque [Nm]
ω_e	Engine rotational velocity [rad/s]
c_m	Mean piston velocity [m/s]
p_{me}	Mean effective pressure [N/m ²]
p_{me0}	Mean effective pressure, mechanical losses [N/m ²]
p_i	Adapted coefficient $i = 1, 2, 3$ [N/m ²]
e_i	Adapted coefficient $i = 1, 2, 3$ [*]

5.3 Motor and Generator

The efficiency, η_i , is describing the losses from the input power to the output power, this is shown in equation (5.9) for the motor and generator. In [6] a similar model is presented.

$$\eta_i P_{in,i} = P_{out,i} = T_i \omega_i \tag{5.9}$$

Power that is required from motor and generator at a certain angular velocity and torque then becomes:

$$P_{in,i} = \frac{T_i \omega_i}{\eta_i} \quad i = m, g \tag{5.10}$$

The electrical prime movers are alternators, i.e. can both work as generator and motor. Values to η_i is provided from look-up tables.

$$P_{in,i} = T_i \omega_i \eta_i^{-sign(T_i)} \quad i = m, g \tag{5.11}$$

Notation for motor and generator

η_i	Motor and generator efficiency [°]
T_i	Motor and generator torque [Nm]
ω_i	Motor and generator angular velocity [rad/s]

5.4 Battery

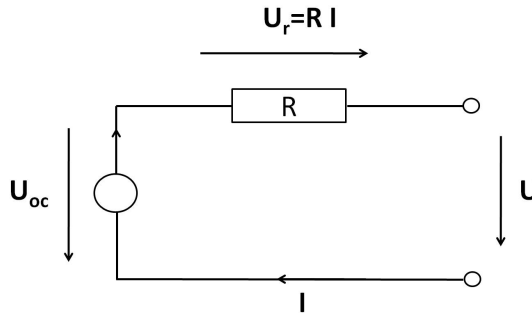


Figure 5.2. Battery is modeled as a resistive circuit with a voltage source.

The model in this section is from [6] and the parameters values are adapted to a battery with a capacity of 6 [kWh]. The battery is modeled as an open circuit with a voltage source in series with a resistance. Applying Kirchoff's voltage law, defined as (5.12), the circuit in figure 5.2 results in (5.13).

$$0 = \sum_i^n U_i \tag{5.12}$$

$$0 = U(t) + U_r - U_{oc} = U(t) + RI(t) - U_{oc} \quad (5.13)$$

Multiplying above equation with U , and using that $P(t) = U(t)I(t)$, the quadratic equation below is obtained. The power in/out of the system is determined by auxiliary, motor and generator, $P(t) = U(t)I(t) = P_{aux}(t) + P_m(t) + P_g(t)$.

$$0 = U(t)^2 + RU(t)I(t) - U(t)U_{oc} \implies U(t) = \frac{U_{oc} - \sqrt{U_{oc}^2 - 4RP(t)}}{2} \quad (5.14)$$

The batteries energy level is often described with its state of charge, SOC. This is the ratio of current and maximum electric charge that defines the dimensionless variable $q(t)$.

$$q(t) = \frac{Q(t)}{Q_0} \text{ with } \begin{cases} \dot{Q}(t) = -I(t) , \text{ discharging} \\ \dot{Q}(t) = -\eta_c I(t) , \text{ charging} \end{cases} \quad (5.15)$$

Because no battery data is available, columbic losses during charging is disregarded, consequently $\eta_c = 1$. Assuming constant resistance in the circuit, the equation (5.15) and with Ohm's law, the voltage U , is re-written as: (5.16).

$$U(t) = RI(t) = -R \frac{dQ(t)}{dt} = -RQ_0 \frac{dq}{dt} \quad (5.16)$$

Inserting (5.16) in (5.13) yields:

$$\frac{dq}{dt} = -\frac{U_{oc} - \sqrt{U_{oc}^2 - 4RP(t)}}{2RQ_0} \quad (5.17)$$

The fact that the U_{oc} depends on the SOC is not considered.

Battery

Q_0	Maximum battery capacity [Ah]
R	Battery resistance [Ω]
U_{oc}	Voltage from voltage source [V]
U	Voltage from voltage source [V]
U_r	Voltage over resistance [V]
I	Circuit current [A]
q	State of charge, SOC [*]

5.5 Drive train

In this section, modeling of the dynamic parts is discussed, values of parameters are both provided by Tianjin University and for the planetary gear set parameters is from [4]. The resulting non-linear state space model is not presented. Due to the complexity of the equation system, assistance of the software Maple is required. A Simulink function called S-Function Builder is utilized to realize the nonlinear state space model that is summarized in 5.5.4.

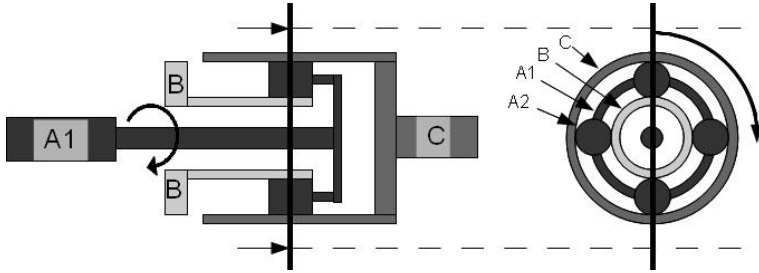


Figure 5.3. A1 and A2 are planetary carrier and gears, B the sun, and C the ring.

5.5.1 Planetary gear set

This thesis project has hybrid architecture consistent with the first Toyota Hybrid System, which also is found in Toyota Prius 1997-2003. Figure 5.3 illustrates the planetary gear set, called PGS, where positive orientation is defined as clockwise. The engine, torque coupler and generator shaft are connected to the planetary carrier, ring and sun. Internal forces on the planetary gear is assumed as equation

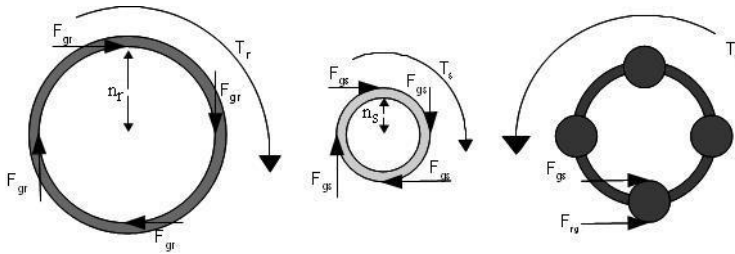


Figure 5.4. Free body diagram of the mechanical parts of the PGS. From the right in the figure are ring, sun and planetary carrier with the planetary gears shown. F is denoting force, T torque and n radius.

(5.18). The planetary gear is also assumed massless. Further the PGS, is assumed not to have any friction losses, it accordingly works as an ideal mechanic component which distributes power. Euler moment law lead to relationship (5.19), (5.20) and (5.21).

$$F = F_{ij} = -F_{ji} \tag{5.18}$$

$$J_r \dot{\omega}_r = -T_r + n_r F \tag{5.19}$$

$$J_s \dot{\omega}_s = -T_s + n_s F \tag{5.20}$$

$$J_c \dot{\omega}_c = T_c - n_r F - n_s F \tag{5.21}$$

Engine and generator connects to the planetary gear shaft and sun shaft. Generator torque is defined as negative compared to the rings rotation. A service brake is

mounted on the shaft, leading to a brake torque T_b , occurs in the equation (5.22).

$$J_e \dot{\omega}_e = T_e + T_b - T_c \quad (5.22)$$

$$J_g \dot{\omega}_g = T_s - T_g \quad (5.23)$$

Hence the engine and generator is direct connected to the planetary carrier and sun, the angular velocity is consequently the same, i.e. $\omega_e = \omega_c$ and $\omega_g = \omega_s$. Eliminating the torque variables T_s and T_c with the relationship (5.22) and (5.23) lead to (5.24) and (5.25).

$$(J_e + J_c) \dot{\omega}_e = T_e + T_b - (n_r + n_s)F \quad (5.24)$$

$$(J_g + J_s) \dot{\omega}_g = n_s F - T_g \quad (5.25)$$

5.5.2 Torque Coupler and final drive

Remaining work is to connect the ring shaft with the motor, torque coupler, final drive and wheel. The figure 5.5 shows the shafts connections. Final drive is

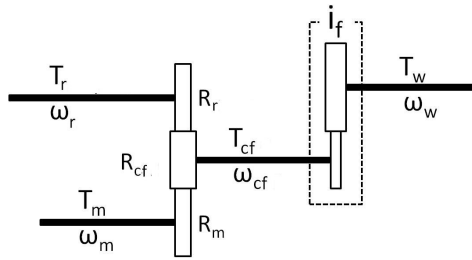


Figure 5.5. Overview of the torque coupler and the final drive.

considered massless and identical ratio in the torque coupler is assumed, i.e. $R_r = R_{cf} = R_m$. This further simplifies calculations.

$$\omega_w = -i_f \omega_{cf} \quad (5.26)$$

$$i_f T_w = -T_{cf} \quad (5.27)$$

$$\omega_r = -\omega_{cf} \quad (5.28)$$

$$\omega_m = -\omega_{cf} \quad (5.29)$$

$$T_{m,out} = T_m - J_m \dot{\omega}_m \quad (5.30)$$

$$J_{cf} \dot{\omega}_{cf} = -T_{cf} + T_{m,out} + T_r \quad (5.31)$$

Inserting (5.26)-(5.30) in (5.31) lead to the relationship (5.32) for the torque converter and final drive. The torque converter is also assumed to be massless.

$$\frac{J_m}{i_f} \dot{\omega}_w = i_f T_w + T_m + T_r \quad (5.32)$$

Further, T_r is eliminated by (5.19) and concludes in the final relationships below, together with the longitudinal vehicle model (5.41), becoming the systems differential equation. The PGS components are always connected, which results in the kinematic constrains in (5.36). This concludes in that the system has two degrees of freedom, hence two states has to be controlled, the third state can not freely be chosen.

$$\frac{(J_m + J_r)}{i_f} \dot{\omega}_w = i_f T_w + T_m + n_r F \quad (5.33)$$

$$(J_e + J_c) \dot{\omega}_e = T_e + T_b - (n_r + n_s) F \quad (5.34)$$

$$(J_g + J_s) \dot{\omega}_g = n_s F - T_g \quad (5.35)$$

$$n_r \omega_m + n_s \omega_g = (n_s + n_r) \omega_e \quad (5.36)$$

To be consistent with section 5.5.3 the wheels angular velocity is also used in this section. Thus, with $i_f \omega_m = \omega_w$ the wheels angular velocity can be re-written to the motors angular velocity.

Notation for torque coupler, final drive and PGS.

F	Internal forces in PGS [N]
J_r	Ring of PGSs inertia [kg m ²]
J_s	Sun of PGSs inertia [kg m ²]
J_c	Carrier of PGSs inertia [kg m ²]
J_e	Engine inertia [kg m ²]
J_m	Motor inertia [kg m ²]
J_g	Generator inertia [kg m ²]
n_r	Inner diameter for the ring in PGSs [m]
n_s	Inner diameter for the sun in PGSs [m]
i_f	Final drive ratio [*]
T_r	Ring torque [Nm]
T_s	Sun torque [Nm]
T_c	Carrier torque [Nm]
T_e	Engine torque [Nm]
T_m	Motor torque [Nm]
T_g	Generator torque [Nm]
T_w	Wheel torque [Nm]
T_{cf}	Torque and final drive torque [Nm]
ω_e	Engine angular velocity [rad/s]
ω_g	Generator angular velocity [rad/s]
ω_m	Motor angular velocity [rad/s]

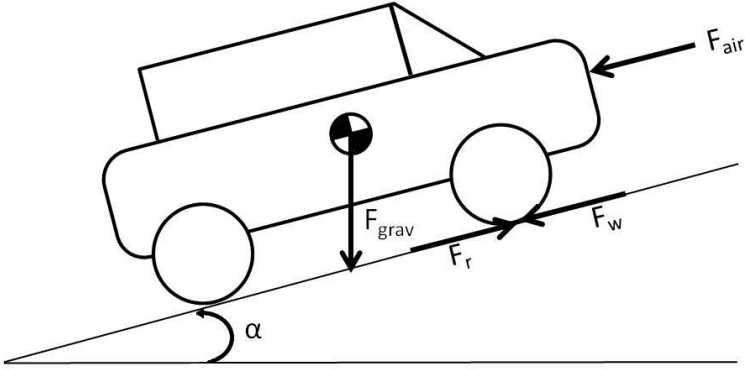


Figure 5.6. Only longitudinal forces are considered, which is referred to as a longitudinal vehicle model.

5.5.3 Longitudinal vehicle model

The dynamic equation for the vehicle obtained with Euler's first and second law.

$$J_w \frac{d\omega_w}{dt} = T_w - r_w F_w \quad (5.37)$$

$$m_v \frac{dv_v}{dt} = F_w - F(v) \quad (5.38)$$

$$F(v) = F_r(v) + F_{air}(v) + F_{grav} \quad (5.39)$$

$$v_v = r_w \omega_w \quad (5.40)$$

With the equation (5.37), (5.38), (5.39) and (5.40) becomes (5.41), which describe the vehicle dynamics.

$$\left(m_v r_w^2 + J_w \right) \frac{d\omega_w}{dt} = T_w - r_w \left(F_r(v) + F_{grav} + F_{air}(v) \right) \quad (5.41)$$

Subject to equation (5.42)-(5.44) from [12], with the assumption $c_1 = 0$, the rolling resistances force becomes a constant.

$$F_r(v) = F_r = m_v g \cos(\alpha) (c_0 + c_1 v_v^2) = m_v g \cos(\alpha) c_0 \quad (5.42)$$

$$F_{air}(v) = \frac{1}{2} \rho_{air} c_d A_f v_v^2 \quad (5.43)$$

$$F_{grav} = m_v g \sin(\alpha) \quad (5.44)$$

Notation for longitudinal vehicle model

J_w	Wheel inertia [kg m ²]
r_w	Wheel radii [m]
m_v	Vehicle mass [kg]
c_d	Vehicle drag coefficient [*]
A_f	Vehicle front area [m ²]
ρ_{air}	Air density [kg/m ³]
g	Standard gravity [N/kg]
c_0	Rolling resistance coefficient [*]
c_1	Rolling resistance coefficient [*]
T_w	Wheel torque [Nm]
F_w	Wheel force [N]
F_{air}	Air resistance force [N]
F_{grav}	Graviton force [N]
F_r	Rolling resistance force [N]
α	Road inclination [rad]
v_v	Vehicle velocity [m/s]
ω_w	Wheel angular velocity [rad/s]

5.5.4 Dynamic Model

The complete powertrain model is then written as equation (5.45).

$$\begin{pmatrix} \dot{\omega}_m \\ \dot{\omega}_e \end{pmatrix} = \begin{pmatrix} a_m T_m + a_e T_e + a_b T_b + a_g T_g + r_1 \omega_m \\ b_m T_m + b_e T_e + b_b T_b + b_g T_g + r_2 \omega_m \end{pmatrix} \quad (5.45)$$

The coefficients a_i , b_i and r_i is lumped parameters from sections 5.5.1 -5.5.3.

5.6 Driver

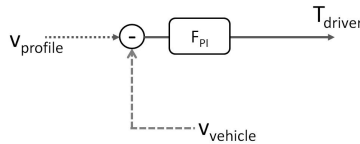


Figure 5.7. A driver is realized by a feed-back PI-controller. Long dashed arrow is current velocity from the vehicle and short dashed arrow is the velocity from the drive cycle.

The torque sum of all prime movers should be equal to the desired torque from the driver acting on the wheels. Due to the different gear ratio between the engine, motor and generator, the coefficient obtained from the dynamic equation determine the constraint that the controller is required to fulfill.

$$T_{driver} = \vec{a}\vec{u} = a_m T_m + a_e T_e + a_b T_b + a_g T_g \quad (5.46)$$

The equation (5.46) describe driver's demanded torque and that the controlled variables, \vec{u} , with the coefficient, \vec{a} , requires to fulfill this demand. The coefficients is obtained from the first row in the dynamic equation (5.45). These coefficients describe the torque from engine, service brake, motor and generator impact on the wheel.

Chapter 6

Supervisory Control System

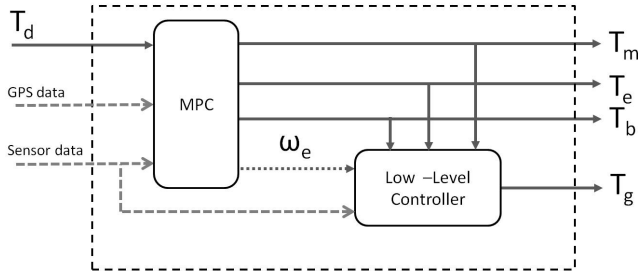


Figure 6.1. The developed supervisory control system consists of two parts, one MPC block and a low level block. Desired torques are solid arrows, long dashed arrows are data and requested angular speed for the engine are the short dashed arrow.

The supervisory control system is divided in two parts, seen in figure 6.1. The MPC block calculates the desired torque to engine, service brake and motor that minimizes the utilization of fuel and divergence from SOC reference. The MPC block provides the low level block with the desired angular speed of the engine. Depending on the engine torque a rule based strategy send a reference angular speed to the low level controller.

6.1 The plant model

$$\dot{\vec{x}} = \begin{bmatrix} \dot{q} \\ \dot{m}_f \\ \dot{\omega}_m \end{bmatrix} = \begin{bmatrix} -\frac{U_{oc} - \sqrt{U_{oc}^2 - 4(P_m(T_m, \omega_m) - P_g(T_g, \omega_g) + P_{aux})}}{2RQ_0} \\ V_d \frac{p_{me}(T_e) + p_{me0}(c_m(\omega_e))}{q_{thv} e(c_m(\omega_e))} \\ a_e T_e + a_b T_b + a_m T_m + a_g T_g + r_1 \omega_m \end{bmatrix} \quad (6.1)$$

Proceeding from the modeling in chapter 5, the non-linear state space model for the states SOC, motor angular speed and the fuel mass are denoted as q , ω_m and

m_f . The matrices in (6.2) are the variables that are used in this thesis. The disturbance is denoted as \vec{v} , the control variable as \vec{u} and the states as \vec{x} .

$$\vec{x} = \begin{bmatrix} q \\ m_f \\ \omega_m \end{bmatrix}, \vec{u} = \begin{bmatrix} T_m \\ T_e \\ T_b \end{bmatrix}, \vec{v} = \begin{bmatrix} T_g \\ \omega_g \\ \omega_e \end{bmatrix} \quad (6.2)$$

6.2 Model Predictive Control

6.2.1 Linearization

From the section 6.1 the model

$$\dot{\vec{x}} = \begin{bmatrix} \dot{q} \\ \dot{m}_f \\ \dot{\omega}_m \end{bmatrix} = \begin{bmatrix} f_1(T_m, T_g, \omega_m, \omega_g) \\ f_2(T_e, \omega_e) \\ f_3(T_e, T_b, T_m, T_g, v_v) \end{bmatrix} \quad (6.3)$$

The MPC block calculates the controlled variables, T_m , T_e and T_b , as illustrated in figure 6.1. With a first order Taylor series expansion a linear state space model is obtained as (6.5). An example of a first order Taylor expansion with a arbitrary parameter ξ is shown in (6.4).

$$f(\xi) \approx f_0(\xi_0) + \frac{df(\xi_0)}{d\xi_0}(\xi - \xi_0) \quad (6.4)$$

The nonlinear state space approximation becomes:

$$\begin{aligned} \dot{\vec{x}}(t) &\approx \vec{f}_0 + A_c(\vec{x} - \vec{x}_0) + B_c(\vec{u} - \vec{u}_0) + E_c(\vec{v} - \vec{v}_0) = \\ &= A_c\vec{x} + B_c\vec{u} + E_c\vec{v} + \vec{f}_0 - A_c\vec{x}_0 + B_c\vec{u}_0 + E_c\vec{v}_0 = \\ &= A_c\vec{x}(t) + B_c\vec{u}(t) + E_c\vec{v}(t) + \vec{F}_c \end{aligned} \quad (6.5)$$

where:

$$\vec{f}_0 = \begin{bmatrix} f_1(\omega_{m0}, T_{m0}, T_{g0}, \omega_{g0}) \\ f_2(\omega_{e0}, T_{e0}, T_{g0}) \\ f_3(T_{m0}, T_{e0}, T_{b0}, T_{g0}, \omega_{m0}) \end{bmatrix}, A_c = \begin{bmatrix} 0 & 0 & \frac{\partial f_1}{\partial \omega_{m0}} \\ 0 & 0 & 0 \\ 0 & 0 & \frac{\partial f_3}{\partial \omega_{m0}} \end{bmatrix} \quad (6.6)$$

$$B_c = \begin{bmatrix} \frac{\partial f_1}{\partial T_{m0}} & 0 & 0 \\ 0 & \frac{\partial f_2}{\partial T_{e0}} & 0 \\ \frac{\partial f_3}{\partial T_{m0}} & \frac{\partial f_3}{\partial T_{e0}} & \frac{\partial f_3}{\partial T_{b0}} \end{bmatrix}, E_c = \begin{bmatrix} \frac{\partial f_1}{\partial T_{g0}} & \frac{\partial f_1}{\partial \omega_{g0}} & 0 \\ 0 & 0 & \frac{\partial f_2}{\partial \omega_{e0}} \\ \frac{\partial f_3}{\partial T_{g0}} & 0 & 0 \end{bmatrix} \quad (6.7)$$

6.2.2 Discretization

Realizing a controller requires a discrete state space model. Assuming the control signal is constant between sampling, i.e. zero-order hold, the discrete system matrices are obtained through (6.8).

$$A_d = e^{A_c T_s}, B_d = \int_0^{T_s} e^{A_c T_s} B_c dt, E_d = \int_0^{T_s} e^{A_c T_s} E_c dt, \vec{F}_d = \int_0^{T_s} e^{A_c T_s} \vec{F}_c dt \quad (6.8)$$

Which results in:

$$\bar{x}[k+1] = A_d \bar{x}[k] + B_d \bar{u}[k] + E_d \bar{v}[k] + \tilde{F}_d \quad (6.9)$$

The remaining problem of calculating the discrete matrices can be done with (6.10). Further explanation is found in [3] and [9]. The usage of the S matrix is done to simplify (6.8) to (6.11).

$$S = \int_0^{T_s} e^{A_c T_s} dt = \mathbf{I} T_s + A_c \frac{T_s^2}{2!} + A_c^2 \frac{T_s^3}{3!} + \dots + A_c^k \frac{T_s^{k+1}}{(k+1)!} \quad (6.10)$$

Since the matrices A_c , B_c , E_c and \tilde{F}_d are time independent they simply become (6.11).

$$A_d = \mathbf{I} + A_c S, \quad B_d = B_c S, \quad E_d = E_c S \quad \text{and} \quad \tilde{F}_d = \tilde{F}_c S \quad (6.11)$$

In the Matlab environment the discrete matrices are instead obtained by the command:

`SYSD = C2D(SYSC, Ts, METHOD)`

The relationship (6.10) and (6.11) has to be used if the Matlab command is not available. The command is used with a zero-order hold method, since in this thesis the Matlab command is available.

6.2.3 Augmented model

In order to remove the constant terms that occur due to linearization the model is augmented. By subtracting the previous state from the current state, influence of constant terms vanish.

$$\begin{aligned} \Delta \bar{x}[k+1] &= \bar{x}[k+1] - \bar{x}[k] \\ \Delta \bar{u}[k] &= \bar{u}[k] - \bar{u}[k-1] \\ \Delta \bar{v}[k] &= \bar{v}[k] - \bar{v}[k-1] \end{aligned} \quad (6.12)$$

$$\begin{aligned} \Delta \bar{x}[k+1] &= A_d \Delta \bar{x}[k] + B_d \Delta \bar{u}[k] + E_d \Delta \bar{v}[k] + \tilde{F}_d - \tilde{F}_d \\ &= A_d \Delta \bar{x}[k] + B_d \Delta \bar{u}[k] + E_d \Delta \bar{v}[k] \end{aligned} \quad (6.13)$$

The SOC, with variable name q , is required to follow a reference, to make this possible augmenting the state space model with an integrator is required. All the states are measurable in the simulation environment. By renaming the variables and matrices in equation (6.14) the final plant model is written as (6.15).

$$\underbrace{\begin{bmatrix} \Delta \bar{x}[k+1] \\ \bar{y}[k+1] \end{bmatrix}}_{= \mathbf{x}[k+1]} = \underbrace{\begin{bmatrix} A_d & \mathbf{0}^T \\ C A_d & \mathbf{I} \end{bmatrix}}_{= \mathbf{A}} \underbrace{\begin{bmatrix} \Delta \bar{x}[k] \\ \bar{y}[k] \end{bmatrix}}_{= \mathbf{x}[k]} + \underbrace{\begin{bmatrix} B_d \\ C B_d \end{bmatrix}}_{= \mathbf{B}} \underbrace{\Delta \bar{u}[k]}_{= \mathbf{u}[k]} + \underbrace{\begin{bmatrix} E_d \\ C E_d \end{bmatrix}}_{= \mathbf{E}} \underbrace{\Delta \bar{v}[k]}_{= \mathbf{v}[k]} \quad (6.14)$$

$$\begin{aligned} \bar{x}[k+1] &= A \bar{x}[k] + B \bar{u}[k] + E \bar{v}[k] \\ \bar{y}[k] &= C \bar{x}[k] \end{aligned} \quad (6.15)$$

Notation of the implemented variables becomes:

$$\vec{x}[k] = \begin{pmatrix} \Delta q[k] \\ \Delta m_f[k] \\ \Delta \omega_m[k] \\ q[k] \\ m_f[k] \\ \omega_m[k] \end{pmatrix}, \quad \vec{u}[k] = \begin{pmatrix} \Delta T_m[k] \\ \Delta T_e[k] \\ \Delta T_b[k] \end{pmatrix}, \quad \vec{v}[k] = \begin{pmatrix} \Delta T_g[k] \\ \Delta \omega_g[k] \\ \Delta \omega_e[k] \end{pmatrix} \quad (6.16)$$

$$\vec{y}[k] = \begin{pmatrix} \Delta m_f[k] \\ q[k] \end{pmatrix}, \quad \vec{r}[k] = \begin{pmatrix} 0 \\ q^{ref}[k] \end{pmatrix} \quad (6.17)$$

6.2.4 Quadratic Programming

$$\vec{u}_{tot} = \sum_{p=0}^{t_c} \vec{u}_p \quad (6.18)$$

The control signal that is calculated in this section is added together, as shown in equation (6.18), in order to obtain the desired torque from the engine, motor and brake. As shown in equation (6.16), is \vec{u} the increment of the torque. This requires the usage of equation (6.18), to obtain the demanded torques. The t_c is the current time, \vec{u}_p is the calculated signal at time p. This sum is calculated after every time the algorithm is used.

Quadratic programming is selected to solve the optimization problem subject to minimizing deviation from a reference. For each sample time, k , a general cost function is expressed as (6.20), constraints as (6.21) subjected to a plant model as (6.22). The weighting coefficients are written as (6.19). The Q_2 is used to weight the control variable, by w_i , $i = 3, 4, 5$. By punishing \vec{u} , jerky behavior can be avoided from the engine and motor.

$$Q_1 = \begin{pmatrix} w_1 & 0 \\ 0 & w_2 \end{pmatrix} \quad \text{and} \quad Q_2 = \begin{pmatrix} w_3 & 0 & 0 \\ 0 & w_4 & 0 \\ 0 & 0 & w_5 \end{pmatrix} \quad (6.19)$$

$$\min_{\vec{u}} z(\vec{u}) = \min_{\vec{u}} \sum_{k=T_0}^{T_0+N_p} \left(Q_1 \left\| \vec{y}[k] - \vec{r}[k] \right\|^2 + Q_2 \left\| \vec{u}[k] \right\|^2 \right) \quad (6.20)$$

$$\vec{\gamma}_u^{min} \leq M_u \vec{u}[k] \leq \vec{\gamma}_u^{max} \quad (6.21)$$

$$\vec{\gamma}_y^{min} \leq M_y \vec{y}[k] \leq \vec{\gamma}_y^{max}$$

$$\text{Subject to: } \begin{cases} \vec{x}[k+1] &= A\vec{x}[k] + B\vec{u}[k] + E\vec{v}[k] \\ \vec{y}[k] &= C\vec{x}[k] \end{cases} \quad (6.22)$$

An example of a two step open loop predictor, accomplish with recursive use of the plant model is shown in (6.23). This means that the first step of prediction is

used for the second and both the first and second prediction is used in the third. Therefore knowledge of the current states and the disturbances is needed to obtain a system where the decision-variables control the future states. In this thesis the disturbances are assumed to be constant over time.

$$\begin{aligned}\bar{x}[k+1] &= A\bar{x}[k] + B\bar{u}[k] + E\bar{v}[k] \\ \bar{x}[k+2] &= A\bar{x}[k+1] + B\bar{u}[k+1] + E\bar{v}[k+1] = \\ &= A^2\bar{x}[k] + AB\bar{u}[k] + B\bar{u}[k+1] + AE\bar{v}[k] + E\bar{v}[k+1]\end{aligned}\quad (6.23)$$

Utilizing the special form above, a general prediction matrix of N_p steps is accomplished in (6.24). The ideas of the equations are from [3]. The matrices are described in equation (6.25)-(6.28).

$$X = \begin{bmatrix} \bar{x}[k] \\ \vdots \\ \bar{x}[k+N_c-1] \end{bmatrix} = \mathcal{A}\bar{x}[k] + \mathcal{B}U + \mathcal{E}V \quad (6.24)$$

$$\mathcal{C} = \begin{bmatrix} C & 0 & \dots & 0 \\ 0 & C & \dots & 0 \\ \vdots & \ddots & \ddots & \vdots \\ 0 & \dots & 0 & C \end{bmatrix}, \mathcal{A} = \begin{bmatrix} I \\ A \\ A^2 \\ \vdots \\ A^{N_p-1}B \end{bmatrix} \quad (6.25)$$

$$\mathcal{B} = \begin{bmatrix} 0 & 0 & 0 & \dots & 0 \\ B & 0 & 0 & \dots & 0 \\ AB & B & 0 & \dots & \vdots \\ \vdots & \ddots & \ddots & \ddots & 0 \\ A^{N_p-2}B & \dots & AB & 0 & 0 \end{bmatrix}, \mathcal{E} = \begin{bmatrix} 0 & 0 & 0 & \dots & 0 \\ E & 0 & 0 & \dots & 0 \\ AE & E & 0 & \dots & \vdots \\ \vdots & \ddots & \ddots & \ddots & 0 \\ A^{N_p-2}E & \dots & AE & 0 & 0 \end{bmatrix} \quad (6.26)$$

This with the vectors:

$$R = \begin{bmatrix} \bar{r}[k] \\ \vdots \\ \bar{r}[k+N_c] \end{bmatrix}, Y = \begin{bmatrix} \bar{y}[k] \\ \vdots \\ \bar{y}[k+N_c] \end{bmatrix} \quad (6.27)$$

$$X = \begin{bmatrix} \bar{x}[k+1] \\ \vdots \\ \bar{x}[k+N_c] \end{bmatrix}, U = \begin{bmatrix} \bar{u}[k] \\ \vdots \\ \bar{u}[k+N_c] \end{bmatrix}, V = \begin{bmatrix} \bar{v}[k] \\ \vdots \\ \bar{v}[k+N_c] \end{bmatrix} \quad (6.28)$$

Further the weighting factors are written as (6.29), which makes it possible to write the cost function with the vectors X and U instead of a sum, (6.30).

$$\mathcal{Q}_1 = \begin{bmatrix} Q_1 & 0 & \dots & 0 \\ 0 & Q_1 & \dots & 0 \\ \vdots & \ddots & \ddots & \vdots \\ 0 & \dots & 0 & Q_1 \end{bmatrix}, \mathcal{Q}_2 = \begin{bmatrix} Q_2 & 0 & \dots & 0 \\ 0 & Q_2 & \dots & 0 \\ \vdots & \ddots & \ddots & \vdots \\ 0 & \dots & 0 & Q_2 \end{bmatrix} \quad (6.29)$$

$$\min_{\bar{u}} z(\bar{u}) = (Y - R)^T \mathcal{Q}_1 (Y - R) + U^T \mathcal{Q}_2 U \quad (6.30)$$

$$Y = \mathcal{C}X = \mathcal{C}(\mathcal{A}x[k] + \mathcal{B}U + \mathcal{E}V) \quad (6.31)$$

With (6.30) and (6.31) yields:

$$\min_{\vec{u}} z(\vec{u}) = \left(\mathcal{C}(\mathcal{A}x[k] + \mathcal{B}U + \mathcal{E}V) - R \right)^T \mathcal{Q}_1 \left(\mathcal{C}(\mathcal{A}x[k] + \mathcal{B}U + \mathcal{E}V) - R \right) + U^T \mathcal{Q}_2 U \quad (6.32)$$

By re-formulating the constraints and equation (6.32), the standard quadratic programming form is obtained in the equations (6.33) and (6.34). By formulating Y in terms of U an optimization algorithm can be used to find the optimum values for U . Interesting to note is that the constraints is linear, this means that re-formulation of constraints on Y can be done to fit the framework in section 6.2.6. The constant term that occurs can be removed without effect on the optimal solution.

$$\min_U \frac{1}{2} U^T \mathcal{H}U + f^T U \quad (6.33)$$

$$\Gamma_u^{min} \leq \mathcal{M}_u U \leq \Gamma_u^{max} \quad (6.34)$$

$$\Gamma_y^{min} \leq \mathcal{M}_y Y(U) \leq \Gamma_y^{max}$$

6.2.5 Optimization - Active Set

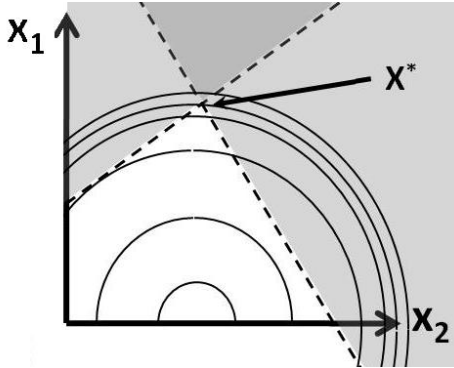


Figure 6.2. The two dashed lines illustrating two constraints, x^* is the optimal value and the solid lines illustrate the topographic of the cost function. The gray area is where no permitted solution can be found. x_1 and x_2 is restricted to only positive values.

The QP Problem is defined as in previous section; the following section describes the algorithm that solves the optimization problem. The figure 6.2 is a geometric illustration of a QP problem. Proceeding from the MPC formulation, and re-writing the problem into only less than inequality, the optimization problem then becomes as (6.35) and (6.36).

$$\min_U \frac{1}{2} U^T \mathcal{H}U + f^T U \quad (6.35)$$

$$\mathcal{M}U \leq \Gamma \quad (6.36)$$

Necessary condition for a non-linear problem to be optimal is the Karush - Kuhn -Tucker conditions, also called KKT condition. With above problem formulation the KKT condition becomes:

$$\begin{aligned} \mathcal{H}U + f^T + \mathcal{M}^T\lambda &= 0 \\ \mathcal{M}U - \Gamma &\leq 0 \\ \lambda^T (\mathcal{M}U - \Gamma) &= 0 \\ \lambda &\leq 0 \end{aligned} \quad (6.37)$$

The active constrains, satisfying $\mathcal{M}U - \Gamma = 0$ for the j :th row, is divided into two sets, the problem becomes (6.38)- (6.42).

$$\mathcal{H}U + f^T + \sum_{j \in S_{act}} \lambda_j \mathcal{M}_j^T = 0 \quad (6.38)$$

$$\mathcal{M}_j U - \Gamma_j \leq 0 \quad j \notin S_{act} \quad (6.39)$$

$$\mathcal{M}_j U - \Gamma_j = 0 \quad j \in S_{act} \quad (6.40)$$

$$\lambda < 0 \quad j \notin S_{act} \quad (6.41)$$

$$\lambda = 0 \quad j \in S_{act} \quad (6.42)$$

Assuming the active set of constraints is known, a closed solution becomes (6.43) and (6.44) which give the optimal solution.

$$\lambda_{act} = -(\mathcal{M}_{act} \mathcal{H}^{-1} \mathcal{M}_{act}^T)^{-1} (\Gamma_{act} + \mathcal{M}_{act} \mathcal{H}^{-1} f) \quad (6.43)$$

$$U^* = -\mathcal{H}^{-1} (f + \mathcal{M}_{act}^T \lambda_{act}) \quad (6.44)$$

6.2.6 Optimization - Hildreth's procedure

Finding the active constraints is done with an active set algorithm called Hildreth's Quadratic Programming Procedure. This method is used due its relatively simple structure and no matrix inversion. The idea of Hildreth's procedure is to identify the constraints that are not active with the dual problem, proceeding with searching on the not active constraints to find a λ that gives the optimal solution. With this vector, which is the Lagrange multiplier called λ , the optimal solution is given by (6.43). The algorithm is only used if there are active constraints, if no constraints are violated, finding the optimal solution can be solved by a least squares method. To guarantee that an optimum is found the problems active constraints have to satisfy:

- Linearly independent.
- Number of active constrains has to be fewer than the optimization variables.

The selection of the control, disturbance and state variables as (6.2) makes that linear independence is accomplished. Number of active constraints is an issue, but the method is still used because the simplicity of Hildreth's procedure. The effect of a violation of this criteria are shown in chapter 7.1, and also how the control variables is affected. Hence Hildreth's procedure is a dual and iterative method, a violation of above requirements will lead to a near-optimal solution. From [11] is the origin of the structures and motivation of utilizing this procedure origin. The vector components in λ are only permitted to vary with one component at each time, λ is defined positive in the direction of the optimal solution. Focusing only on one component, i.e. λ_j , adjusting this component to improve the cost function. If this is not possible without violating the constraints, i.e. negative λ_i , this component is set to zero. By defining (6.45) and denoting p_{ji} as the j :th component in the matrix P and l_j as the j :th component in the vector L . Iterating the i :th component in the λ vector at time n an explicit form is obtained as (6.46) and (6.47).

$$P = \mathcal{M}_{act} \mathcal{H}^{-1} \mathcal{M}_{act}^T, L = \Gamma + \mathcal{M} \mathcal{H}^{-1} f \quad (6.45)$$

$$\lambda_j^{n+1} = \max\{w_j^{n+1}, 0\} \quad (6.46)$$

$$w_j^{n+1} = -\frac{1}{p_{jj}} \left(l_j + \sum_{i=1}^{j-1} p_{ji} \lambda_i^{n+1} + \sum_{i=j+1}^m p_{ji} \lambda_i^n \right) \quad (6.47)$$

The converged vector λ^{con} , either contain a positive value or zero. With a predetermined accuracy, a closed formula is obtained as (6.48). If $\lambda^{con} = 0$ would the expression describe a solution with no active or no constraints. The term $\mathcal{M}^T \lambda^{con}$ is describing the correction term.

$$U^* = -\mathcal{H}^{-1} \left(f + \overbrace{\mathcal{M}^T \lambda^{con}}^{\text{Correction term}} \right) \quad (6.48)$$

Further information about duality and optimization theory is found in [5], and for Hildreth's procedure in [11].

6.3 Low level controller

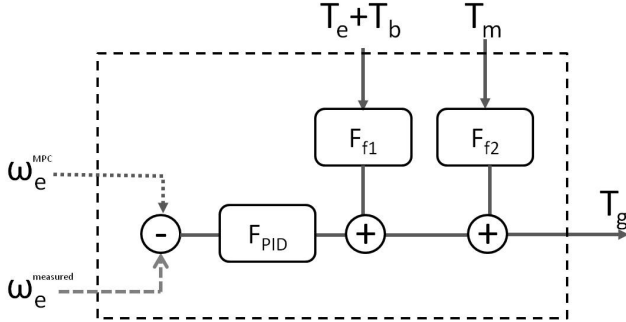


Figure 6.3. The reference angular speed from the MPC block is fed back with the angular speed of the engine, denoted ω_e^{MPC} and $\omega_e^{measured}$ respectively.

The low level controller block contains one PI controller with two feed-forward controllers from the torques demands from the MPC block. The torques demands are regarded as disturbance in the low level controller block, which is natural if the dynamic equation from the powertrain, equation (5.45), is regarded. The figure 6.3 illustrates the different parts of the low level controller. Tuning of the parameters is done with a method called lambda method, found in [3]. Below is a short introduction of the lambda method.

$$F_{PI}(s) = \frac{T_i}{K_p(\lambda T_i + L)} \left(1 + \frac{1}{T_i} \frac{d}{dt}\right) \tag{6.49}$$

The PI controller is described as equation (6.49), and the parameters are adjusted by using the rules in equation (6.50).

$$K = \frac{T}{K_p(\lambda T + L)}, T_i = T \tag{6.50}$$

K_p is the loop gain, L the delay time and T is the time constant. The parameter λ is tuned so the systems rise-time and settling time are acceptable.

Chapter 7

Results

The weighting matrices \mathcal{Q}_1 and \mathcal{Q}_2 are tuned by trial and error and kept constant during all time. The matrices are configured to be charge sustaining and are not particular adapted to any driving cycle. A substantial time was spent on finding the weighting coefficients that are used, further tuning could improve the systems performance but because lack of time this was not done. An increased value of the weight that is punishing the difference between the reference SOC and current SOC would make the system to follow the reference closer, but this would also lead to a higher cost for some driving cycles. \mathcal{Q}_1 and \mathcal{Q}_2 is tuned and is maintained constant for all simulation, this is made to be able to investigate the influence of other parameters and how a model error are affecting the system.

7.1 Step response

Result of a driver desire to accelerate up to 110 [km/h] and maintain this speed until the vehicle is stabilized in CDCS mode is discussed in this section.

As discussed in section 6.2.6; guarantee to find the optimal control variable requires that the number of active constraints must be fewer than the optimization variables. The variables T_m , T_e and T_b are the optimization variables, T_{driver} and T_g are the measurable variables. There are three optimization variables, which leads that only two constraints can be active. During the acceleration phase, the variable T_b is always calculated to zero by the controller because braking the engine's shaft when using the engine would be ineffective. The equation (7.1) is re-writen with $T_b = 0$.

$$\begin{array}{l}
 T_{driver} - a_g T_g = a_m T_m + a_e T_e + a_b T_b \\
 T_e = T_e^{max} \\
 T_m = T_m^{max} \\
 T_e = T_e^{min} \\
 T_m = T_m^{min}
 \end{array}
 \begin{array}{l}
 \xrightarrow{T_b=0} \\
 0 > 110 \text{ [km/h]}
 \end{array}
 \begin{array}{l}
 T_{driver}^{max} - a_g T_g = a_m T_m^{max} + a_e T_e^{max} \\
 T_e = T_e^{max} \\
 T_m = T_m^{max}
 \end{array}
 \tag{7.1}$$

At maximum torque's demands from the driver must all three constraints in equation (7.1) be satisfied. During these circumstances, it is not possible to guarantee

that the algorithm accomplish this. Linear independent and fewer optimization variables than active constraints that are the two criterion that have to be fulfilled, as discussed in section 6.2.6, is violated during these circumstances. Linear independent between the equations are not possible when there are two variables that have to fulfill three equations. In the figure 7.1 and 7.2 is the time marked when the constraints are active. Hildreth's procedure gives with these circumstances a converged solution that makes the solution near optimal. When there are two active constraints this is marked with multiple colors.

7.1.1 Acceleration

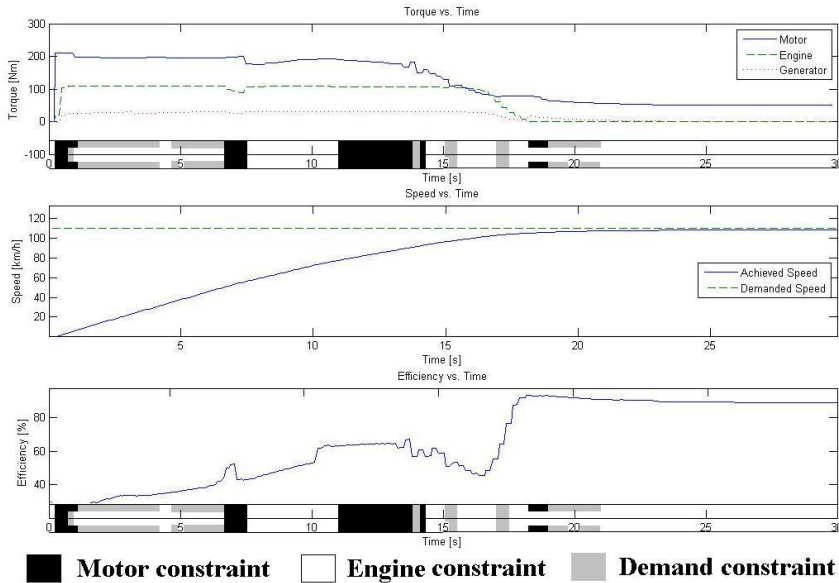


Figure 7.1. The top graph illustrates the torque's demands from the controller to the engine, motor and generator. Overall efficiency and vehicle speed is shown in the other two graphs. The different colors show when different constraints are active.

The figure 7.1 illustrate a driver that desires to accelerate up to 110 [km/h], and after this continuing cruising at this speed. The vehicle is accelerating between 0-20 [s], during this time the motor is assisted by the engine and the generator. The generator work as motor and is providing power to the wheels during this acceleration phase, this is a consequence of the kinetic constraints of the PGS, discussed in 5.5.2, and that the low level controller needs to control the engine angular velocity. The motor is direct connected to the drive shaft; therefore the motor is unable to provide the same torque for higher angular velocity as for lower. This is regarded by the controller, consequently only demanding maximum torque that is possible for the current angular velocity. A closer look at the time interval

15-20 [s] illustrates the motor's decreased torque, and the engine torque remaining 110 [Nm] until 17 [s] before it decreases the torque. When the active constraints are shifted, disturbance from the torque that the engine and motor deliver can occur. This is particularly visible in figure 7.2 at 7.5-15 [s], during this time period is the desired torque from the driver not fulfilled. During the acceleration the overall efficiency are around 40 %, to become 90 % after the acceleration part, when the engine is not required to assist the motor. The overall efficiency increasing when the vehicle speed is increasing, this is shown in 7.1. This is because the motor is direct connected to the wheel through the torque coupler, i.e. the motor's angular velocity is proportional to the wheels' angular velocity. The short increase of efficiency of 9% around 7-7.5[s] is caused by active constraints are shifted, but it is remarkable that it is so significant and during such short time. A better explanation would have been desirable, but due to lack of time deeper analysis where not done.

At 16 [s] reaches the vehicle 100 [km/h], even the desired velocity is not reached, decreases the demanded torque from the driver. The engine's angular velocity can freely be controlled, meaning engine can provide, at all vehicle speeds, 110 [Nm]. In figure 7.1 at 17 [s], the engine's torque decreases despite the reference vehicle velocity is not reached, this since the required torque from the driver is decreased. The figure 7.2 illustrate the decreased torque's demands from the driver. This is because the driver is realized with a PI-controller, where the demanded torque is a function of the difference between the driving cycles reference speed and current vehicle speed.

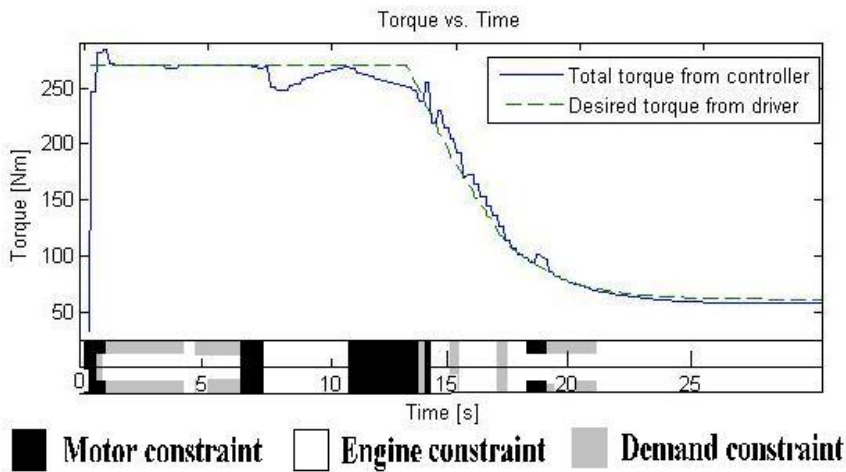


Figure 7.2. Dashed line is the desired torque from the driver and the solid line is the actual torque acting on the wheel.

$$T_{driver} = a_m T_m + a_e T_e + a_b T_b + a_g T_g \quad (7.2)$$

The controller is designed to follow the required torque from the driver. The torque's demands from the driver have to be fulfilled by the controller, where the coefficients a_m , a_e , a_b and a_g in the equation (7.2) are describing the engine's, motor's and generator's torque acting on the wheels. In the figure 7.2, it is showed that the torque from the engine, motor and generator deviates from the desired torque. This is caused by the multiple active constrains.

7.1.2 CDCS

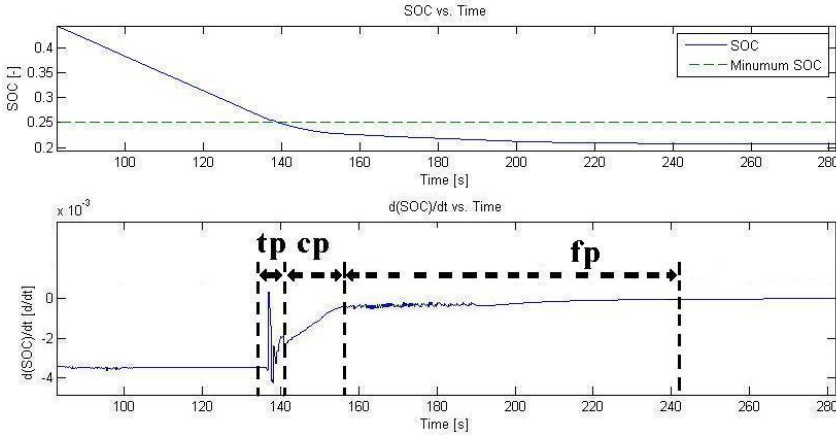


Figure 7.3. Change of strategy from electric drive to CDCS initialize when the SOC passing the reference at 0.25. tp representing the transient phase, cp representing the convergence phase, and fp is the final phase.

In this section the vehicle continues driving with a velocity of 110 [km/h]. Due to the batteries SOC reaches the minimum level, the controller changes strategy in order to be charge sustaining. The CDCS mode consists of three phases, transient, convergence and final phase, illustrated in figure 7.3. In the transient phase the generator provides a negative torque. This because the engine angular velocity requires to be controlled, due to that the engine is engaged. This phase transiently gives rise to a positive derivate of the SOC. The time the low level controller needs to control the engine angular velocity is the same as the time for this phase. After the transient phase, the convergence phase starts, in this phase the SOC almost reaches a stationary value. The MPC is unable to directly control the generator because of the architecture of the designed supervisory control system. The settling time is 73 [s] with an accuracy of 5 %. The settling time is defined as the time it takes to reach a stationary value with a predetermined accuracy. The convergence phase requires the generator to work as a motor, i.e. utilize energy to provide power to the wheel, this in order to control the engine angular velocity. The final phase that makes the usage of battery energy to zero is a long phase where the disturbance of the low level controller is a probable reason why it is so

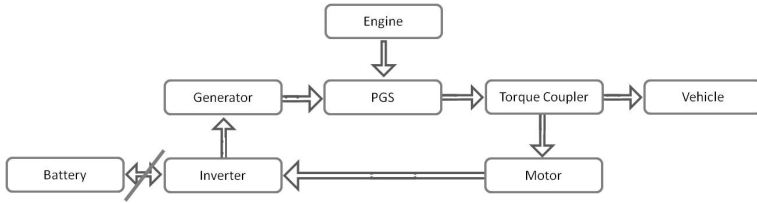


Figure 7.4. The generated energy from motor is utilized by the generator.

long. In summary, all the three prime movers, engine, generator and motor are required to be engaged to maintain charge sustenance. Figure 7.4 illustrates the power path of the system during CDCS mode.

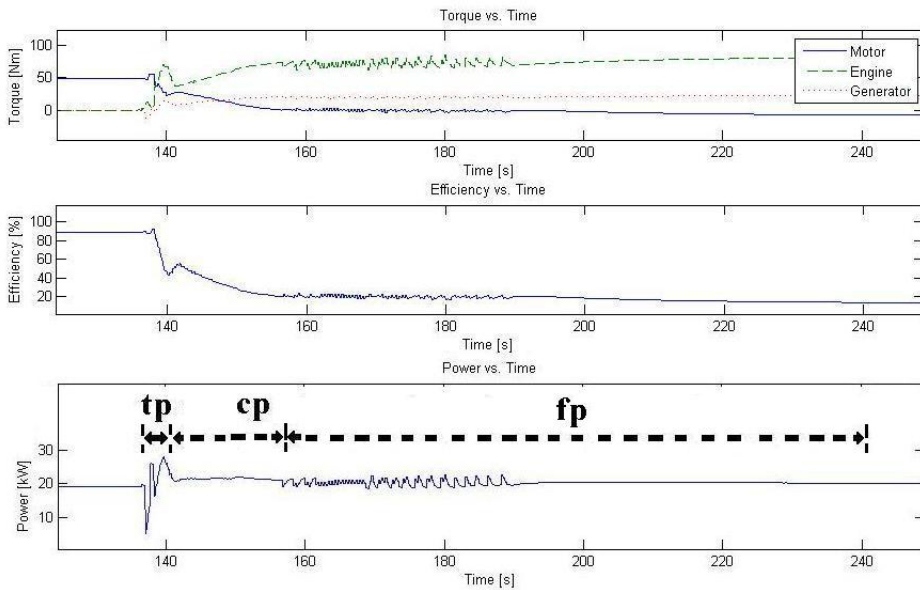


Figure 7.5. The disturbance of the power to the wheel is illustrated in the bottom graph. The solid arrow denoted *tp* is the duration of the transient phase, the dashed arrow denoted *cp* is the converge phase and final phase is denoted as *fp* .

Start of engine is illustrated in figure 7.5, where increased engine and generator torque with decreased motor torque represents change of strategy. The fast decreased power acting on the wheel is derived from the negative generator torque at 136[s]. At this time, the generator is generating power to the battery, for about 1.5 [s] power is re-directed to the battery instead of direct all the power to the

wheel. During this phase, all the power is directed into the generator, i.e. it is charging the battery. The overall efficiency is higher at transient phase compared with the convergence phase, although the power to the wheel is not maintained at necessary level. The oscillations around zero torque at 150-175[s] from the motor are amplified by the engine. The efficiency is affected to start to vary between 15-22%. No reason why the motor's torque began to oscillate around zero are found, but a low pass filter after the MPC controller could dampen those oscillations, but this where not carried out in this work. The figure is showing the effect on the

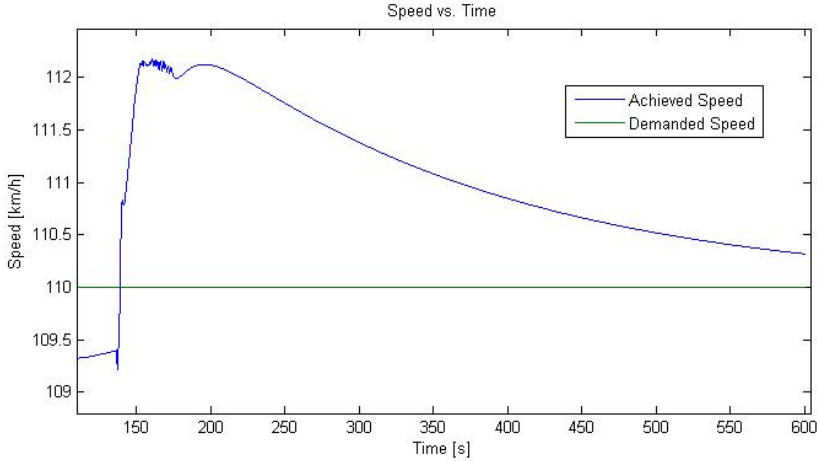


Figure 7.6. The axes scale is enlarged to illustrate the vehicle's insignificant deviation from the reference's velocity.

vehicles velocity when changing mode, during a time period of 18 [s] the velocity of the vehicle increases 2.5 [km/h]. The MPC is disturbed by the low level controller that controls the generator's angular velocity. The MPC represses the disturbance and the speed slowly converge to 110 [km/h], a MPC that handles the disturbance parameter, \vec{v} , faster would be desirable but is not accomplished here.

7.2 Sampling time and control horizon

This section focus on influence of the different design variables; sampling time and control horizon. The weighting matrices, Q_1 and Q_2 , are tuned so the system is charge sustaining and follows the driving cycle, if this is possible. The same value from the beginning of the chapter is used throughout the chapter. Charge sustenance is accomplished by use a high value on SOC deviation coefficient, additionally; a larger value of usage of fuel is used to avoid utilization of fuel. The coefficients are not adapted to any particular driving cycle. An extension of the NEDC driving cycle with an extra highway cycle in the start is used during the simulation, figure 7.7. Criteria for an acceptable simulation are:

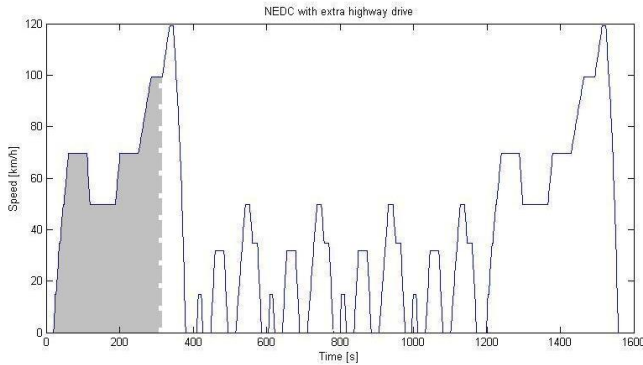


Figure 7.7. Gray is the all electric drive area, where the remaining is in CDSCS mode.

- Follow the driving cycle.
- In the figure 7.7 the gray area is the all electric area. No different in performance is allowed between electric drive and CDSCS drive.
- SOC within 0.25 ± 0.1 .

The ability to follow the reference is considered important. The unknown future torque's demands from the driver causes problem. The controller is using the same desired torque value for the whole prediction time. This causes issues since a change in speed will also become a change on torque's demands. A long prediction horizon is only beneficial when the driving cycle has small variations. The table

Overall efficiency [%]				State of Charge, SOC [-]			
$T_s \setminus N_p$	6	10	15	$T_s \setminus N_p$	6	10	15
0.25 s	-	50.9210	52.7812	0.25 s	-	0.2333	0.2628
1 s	53.1454	54.7715	-	1 s	0.1969	0.2525	-

Table 7.1. The symbol '-' representing simulations where one or more criteria is violated.

7.1 is an example of how the overall efficiency and SOC is influenced by different sampling time and prediction horizon, defined as T_s and N_p . Comparing the different prediction horizons, the table 7.1 illustrates that the overall efficiency and the SOC is higher with a longer prediction horizon. Utilization of electric energy offers great possibility of a high efficiency, and despite the usage of electric energy is higher for the shorter sampling time, the overall efficiency is higher for the long prediction horizon. The proportion for other sampling time and prediction horizon follows the results shown in the tables, but for simplicity they are not presented. The table 7.1 presents the driving cycles end values, whereas the figure 7.8 illustrate the time variation. A longer sampling time allows the SOC to deviate more than a shorter sampling time. A sampling time of 1 [s] causes the controller to

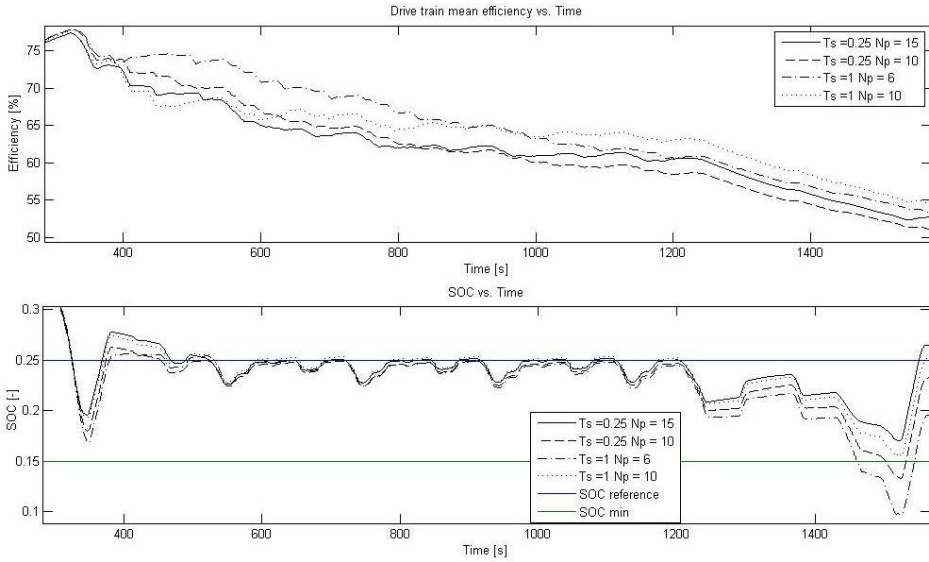


Figure 7.8. Four different set of parameters are presented. The reference and minimum SOC are the horizontal straight lines.

violate the lower bound of the SOC, therefore is not charge sustaining nor robust. A faster sampling time thus results in a more robust controller. During simulation the longer sampling time lead to approximate four times shorter simulation time.

7.3 Robustness

The previous section implicate that the best robustness is with a sampling time of 0.25 [s] and prediction horizon of 15 samples. In this section are these parameters used. The MPC structure used in this thesis does not guarantee stability; therefore it is important to simulate effects from a model error. There are modified MPC that guaranty stability, but for simplicity and lack of time this is not implemented. The controller assumes the vehicle driving on a road with no slopes. Implementing a constant slope of 2° and 1° in the model, but not in the controller, gives implication of how a model error affects the performance. The extended driving cycle, figure 7.7, presented in the previous section, is also used during simulations for this test. The figure 7.9 illustrates the controller's ability to follow the pre-determined extended driving cycle, with a model error. It is important to stress that the vehicle is constantly driving uphill. During the first acceleration part, the vehicle speed with a road of 2° slope is approximate 4 km/h lower than with a horizontal road. According to the simulation, the velocity differences from the horizontal road decreases over time. The first highway phase depletes the battery significantly faster for the simulation with road slope than the horizontal road. Conversion to road slope in percent is; slope of 2° is 3.49 % and 1° is 1.75 %.

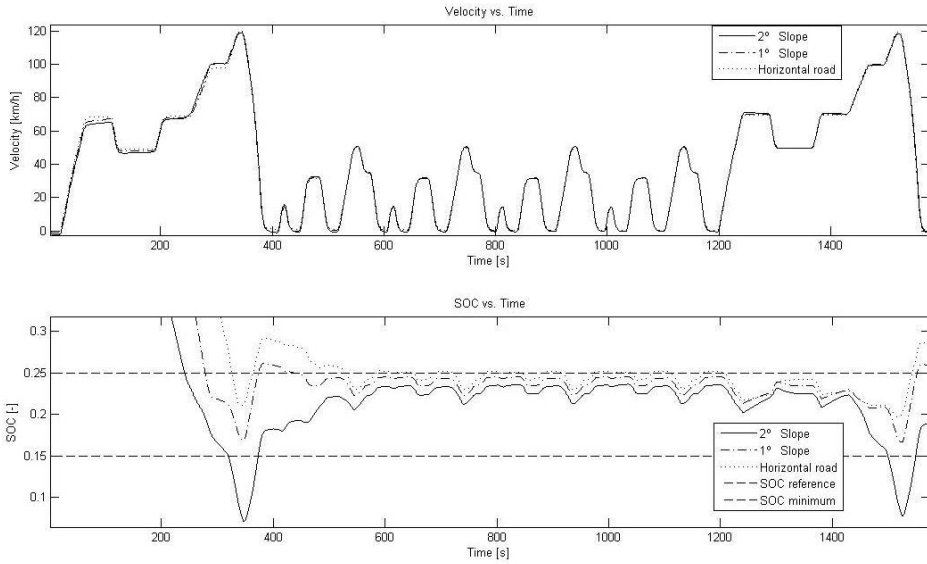


Figure 7.9. The slope of 2° is close to zero at the SOC level, consequently not charge sustaining. The slope of 1° is in the allowed boundaries of the SOC level.

Percent is used on road signs; therefore are this conversion interesting.

7.4 Utilization of GPS

Information of the driving cycles length is provided by the GPS, here defined as d_0 . The vehicles traveled distance is measured and defined as d_m . The equation (7.3), determines the reference SOC, in the equation the SOC is denoted q . The function is linearly decreasing with the lowest value of 0.25. The functions value is permitted to vary ± 0.1 , therefore the lower boundary is 0.15. The term $q^{ini} - q^0$ is the start value of the SOC reference. An initial lower reference than the initial SOC is use to immediate encourage the controller to use the electric energy in the beginning, the controller will later restrict the use of electric energy to encourage blended driving. The driving cycles length is always longer than the all electric range. Use of the fuel is required to extend the vehicles range, if this is not required, engaging the engine becomes unnecessary. GPS information is considered reliable and issues derived from length uncertainty of the cycle are addressed in [10].

$$f(d_m) = \begin{cases} q^{ini} - q^0 - (q^{ini} - q^0 - q^{min}) \frac{d_m}{d_0} & \text{if } 0 \leq d_m \leq d_0 \\ q^{min} & \text{else} \end{cases} \quad (7.3)$$

The percent in the table 7.2 - 7.4 is defined as equation (7.4). This is used to give a overview of the different between blended driving and CDCS driving.

$$\Delta = \frac{CDCS - Blended}{Blended} \quad (7.4)$$

7.4.1 Highway, Urban and City driving

Cycle	CDCS q	Blended q	CDCS Cost	Blended Cost	Δq	Δ Cost
A	0.263	0.293	0.466	0.456	-10.2 %	2.2 %
B	0.244	0.254	2.15	1.99	-3.9 %	8.0 %

Table 7.2. q is the SOC, and a positive % value defines as higher CDCS value compared to the blended value.

The table 7.2 is in line with the conclusion that blended driving can lead to a lower cost. Additional to the lower cost, it is important to stress that the end value of the SOC is higher. When blended driving is used on Cycle A, nearly the entire mission has a higher cost, due to the engine being engaged relative early, see figure 7.10. During CDCS drive the engine is engaged at 5 [km], consequently the controller has to utilize fuel to a higher extent than the blended driving. For cycle A, the difference in cost at city driving section in 7-11[km] maintained constant. Additionally, during this section, the use of the electric energy is higher for the CDCS driving than the blended driving. During the second highway section, the blended driving cost decreases relative to the CDCS driving, and finally result in a lower total cost for the blended driving.

For driving cycle B, blended driving reduces the cost compared to CDCS more than for cycle A. At approximate 30 [km] the cost for blended driving becomes equal to the cost of CDCS driving. Additionally, for this section, the utilization of electric energy is lower with blended driving.

Blended driving reduces the cost for cycle B significant more than blended driving for cycle A.

7.4.2 City driving

Cycle	CDCS q	Blended q	CDCS Cost	Blended Cost	Δq	Δ Cost
C	0.248	0.260	0.194	0.182	-4.6 %	6.6 %
D	0.241	0.256	0.453	0.366	-5.9 %	23.8 %

Table 7.3. q is SOC, and a positive % value defines a higher CDCS value compared to the blended value. A significant cost saving can be made when driving in blended driving for cycle D.

Blended driving is shown to have lower cost for both of the simulated city cycles, as shown in table 7.3. The SOC is also higher at the end of the simulation for the blended driving. Comparing the result between the cycles, D has a significantly greater increase in fuel economy compared to cycle C. On the cycle C the cost for blended driving is almost immediately lower than CDCS, whereas cycle D shows improvement in the end of the cycle. This is illustrated in figure 7.11.

7.4.3 Highway driving

Cycle	CDCS q	Blended q	CDCS Cost	Blended Cost	Δq	Δ Cost
E	0.247	0.261	1.19	1.12	-5.7 %	6.3 %
F	0.219	0.240	1.96	1.89	-9.6 %	3.7 %

Table 7.4. q is referred as SOC, and a positive % value defines as higher CDCS value compared to the blended value.

The result from simulation is shown in table 7.4. CDCS driving in both cycle E and F is using battery energy to a higher extent compared to blended driving. The cost for blended driving in both cycles is lower than CDCS driving. This shows the benefits of blended driving. The cycles E and F present similar result the first half, shown in figure 7.12, where the cost for the blended driving is higher. But as the simulation proceed; the remaining possibility to use electric energy finally leads to a lower overall cost.

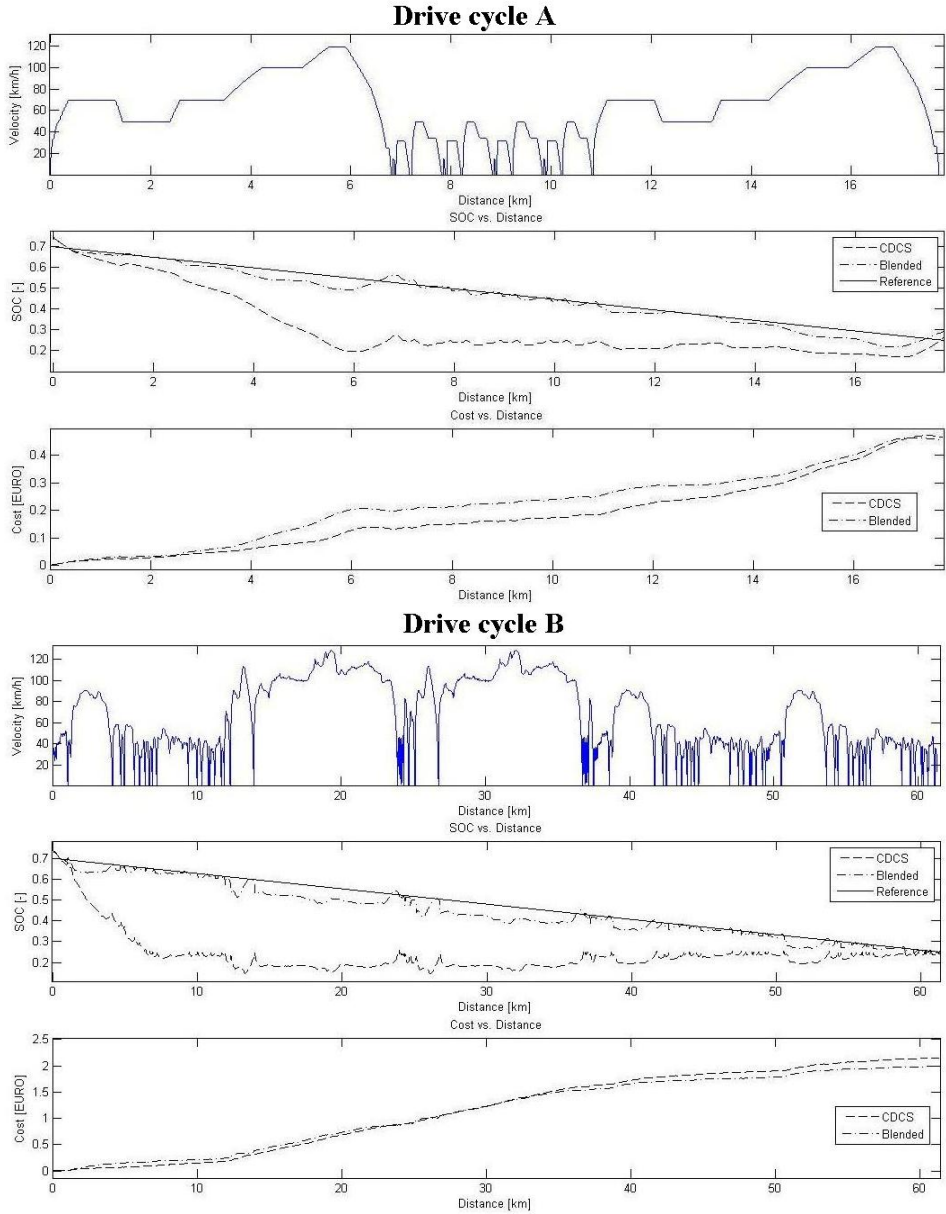


Figure 7.10. The dashed line is CDACS simulation and the dash dotted from the blended simulation.

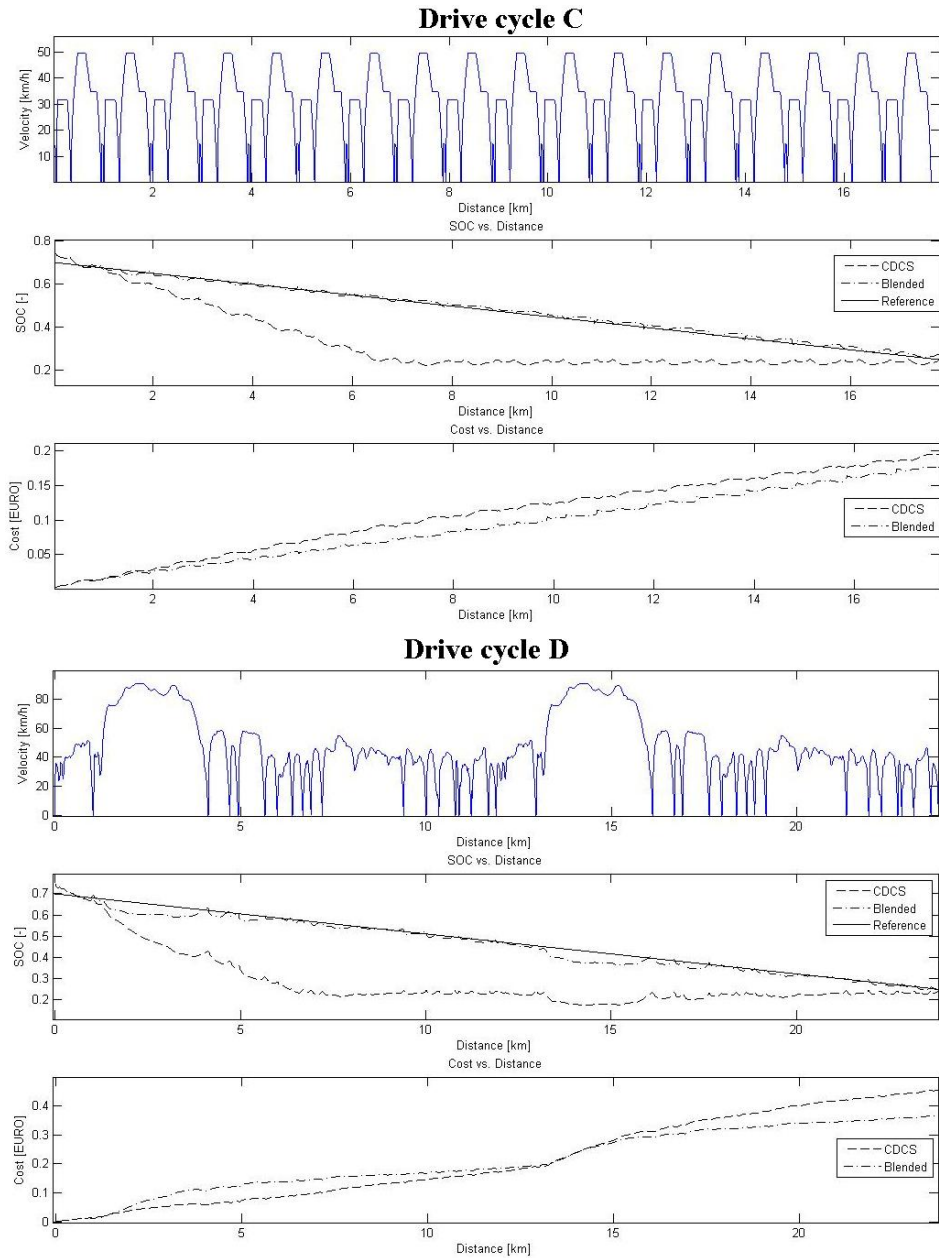


Figure 7.11. The dashed line is representing the result from CDCS simulation, and the dash dotted is the blended simulation.

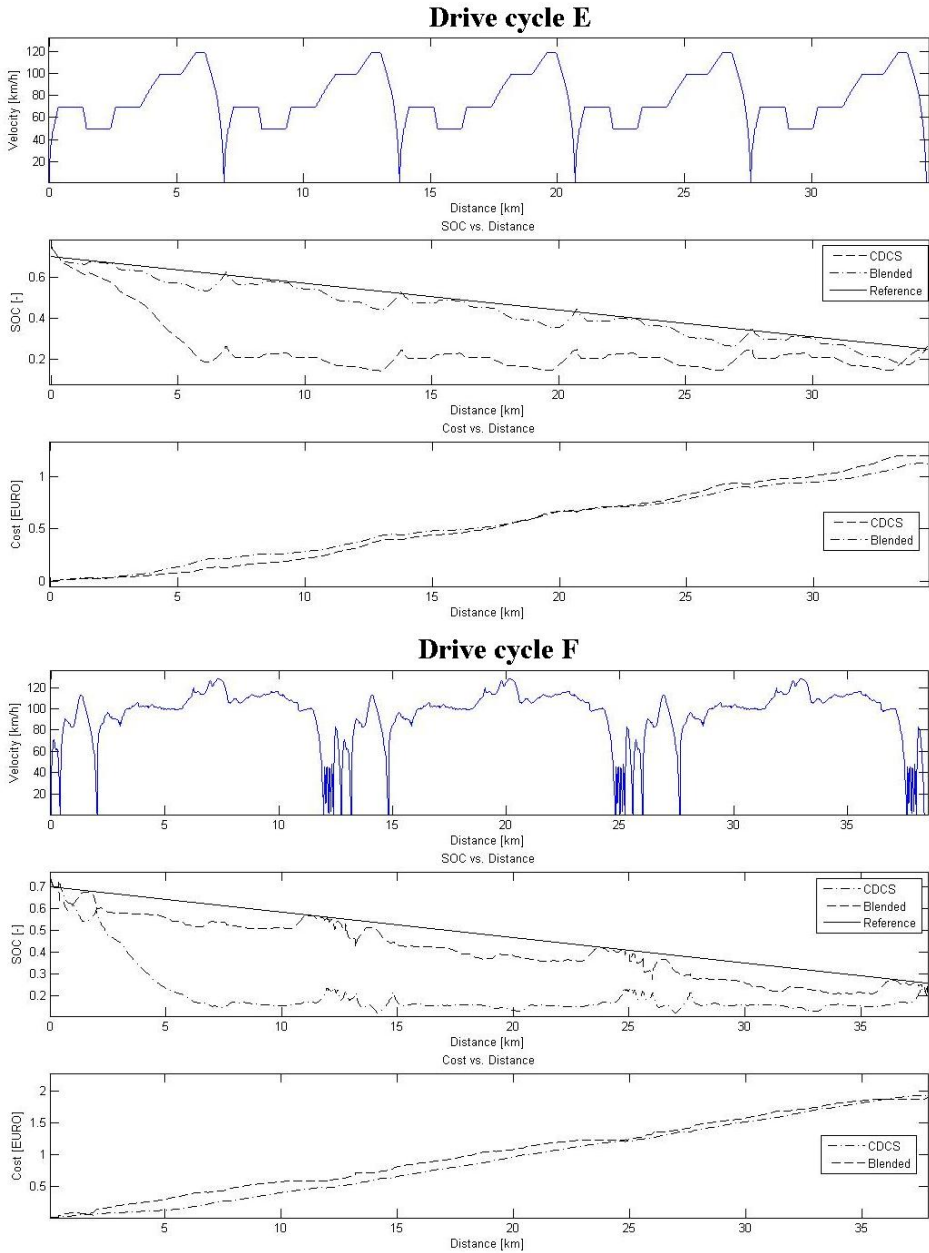


Figure 7.12. In this figure dash dotted line is CDCS driving and the blended driving is dashed lines.

Chapter 8

Conclusions

To solve the problem of blending battery energy with fuel from beginning of a driving cycle a variable SOC reference was developed, which where depending on information from a GPS. Result from the simulation, shows that using blended driving reduce the cost of driving. Some driving cycle's costs is reduced almost 24%. The mean value for the others cycles were around 5%, where they varied between 2.2-8%. The developed supervisory control system has acceptable performance, meaning it follows the driver's torque demands when the circumstances to do so are right, with no model error and a sampling time of 0.25 [s] the system is charge sustaining and considers constraints. The controller can operate in all possible modes, the hybrid mode and only electric mode. The controller also presents robustness against error in the plant model, this for moderate slopes up to 1° , in percent this is $\approx 1.5\%$. Further in this chapter the result discussed more thorough and also topics for future work are presented.

8.1 Step response

The controller can follow the requested torque from the driver for the most of the time, but in some particular cases problems arise. Issues are derived from that the MPC controller uses an active set method. During maximum torque request, limitations from engine, motor and torque request are active, totally three active constraints. The implemented algorithm requires that the active constraints are fewer than the optimization variables, this to guarantee to find the optimal solution. During these circumstances, the number of active constraints are equal the number of optimization variables. This is discussed in section 6.2.6 where the necessary conditions are shown. In the section 7.1 effects on performance are shown. To solve this problem a different method of finding the optimal solution has to be used.

The generator angular speed is a linear combination of engine and motor angular velocity, which is a consequence of the vehicle's configuration, this is addressed in section 5.5.1 and equation (5.36). The active set method is not guaranteed to

find the optimum for problems where linear dependency exists, which is addressed in section 6.2.6. To be able to handle the complexity, the Supervisory Control System is divided into two parts, one MPC structure controller and one low level controller. A disadvantage of this structure is that the MPC block is unable to control the generator. The optimization does not include the generator; further consequence is that a global optimum might not be obtained.

To solve this, an optimal method which handles linear dependency, and ability to consider more active constraints than optimization variables, has to be used.

To completely disengage all electrical prime movers is not possible in this architecture; hence the generator is required to control engine angular velocity. Although when the lower boundary of the SOC is reached, the motor is providing enough of energy to the generator. In this mode all the utilized energy is derived from the fuel. All possible modes can be accomplished with the controller; pure EV mode and hybrid mode.

The structure of the PIHEV when the SOC is at the lowest allowed boundary is similar to a series hybrid. The power to the wheel is derived from the fuel, but a part of the fuel energy is converted to electric energy to control the engine angular velocity.

8.2 Sampling time and control horizon

A short sampling time offer possibilities of a more robust controller. A longer prediction horizon might give a higher overall efficiency than a short. In this thesis the requested torque's demands is considered as a constant during the whole prediction horizon, this could cause issues if the torque's demands from the driver deviates significantly compared to the predicted. A possible improved solution with an observer, that predicts the future desired torque from the driver, could remove the open loop structure. The controller is adjusting the control signal every sampling period, which provides a simulation with acceptable vehicle performance and charge sustaining properties. This requires selecting a sampling time of maximum 0.25 [s].

8.3 Robustness

Slopes up to 2° give reasonable driving performance, although issues of charge sustaining are more visible. Slopes up to 1° is handled by the controller, and provide a simulation that is charge sustaining and follow the driving cycle, but greater slopes cause problems with charge sustaining. Hard constraints on the SOC could solve this problem, but due to insufficient time and issues derived from use of an active set method, this was not carried out.

8.4 Utilization of GPS

The GPS information assist the controller to reduce the cost of driving, which coincide with the result from [10]. It is important to emphasize that the range the vehicle travels is required to be longer than the all electric drive. The six presented drive cycles all indicate positive effects of blended driving. The blended driving could engage the engine more frequently compared to CDCS driving. Heating the engine to optimal temperature might be needed to be done more frequent. This could raise the fuel consumption and consequently increase the cost for the blended driving. This could also increase emissions and greenhouse gases. No extra cost in the cost function is implemented due to the higher emissions a cold engine would cause, which could be a topic for further investigation. Therefore the simulated result could deviate from real tests. Additionally, slower depletion might generate less wear on the battery: this would probably be desirable for testing in reality.

For blended driving all cycles, except of cycle F, has higher SOC end values than the reference value. For blended driving the reference SOC is 0.25 at the end of simulation. Using the electric energy to a higher extent than the presented strategy, might further decrease the overall cost.

8.5 Future work

Unfortunately lack of data and test possibilities, the simulation result could never be verified, which could be a very interesting topic to continue on. Further it would be interesting to obtain the optimal solution, with assistance of DP, to compare the algorithms performance.

A different optimization algorithm, than the Hildreth's procedure, could further improve the system. The method needs to handle multiple active constraints and linear dependent constraints.

The plant model could probably be subjected to simplification; this would probably be desirable in an implementation. Finding suitable linearization points could also reduce the calculation burden.

Imposing hard constraints on the SOC level would also guarantee charge sustaining. Solving this issue is associated with replacing the current active set algorithm. However, a different approach of variable weighting factor for the SOC deviation might be sufficient.

Bibliography

- [1] *Predictive control of drivetrains*, July 2002. 15th Triennial World Congress.
- [2] *A-ECMS: An Adaptive Algorithm for Hybrid Electric Vehicle Energy Management*, December 2005. IEEE Conference on Decision and Control, and the European Control Conference.
- [3] M. Enqvist. *Industriell reglerteknik - Kurskompendium*. December 2008. First Edition.
- [4] A. Vahidi A. M. Phillips M. L. Kuang I.V. Kolmanovsky H. A. Borhan. Predictive energy management of a power split hybrid electric vehicle. June 2009. American Control Conference.
- [5] M. Ronnqvist och P. Varbrand J. Lundgren. *Optimeringslara*. Second Edition.
- [6] A. Sciarretta L. Guzzella. *Vehicle Propulsion Systems, Introduction to Modeling and optimization*. June 2007. Second Edition.
- [7] B.Egardt L.Johannesson, M.Åsbogå rd. Assessing the potential of predictive control for hybrid vehicle powertrains using stochastic dynamic programming. March 2007. IEEE Transactions on intellegent transportations systems.
- [8] G. Rizzoni P. Pisu. A comparative study of supervisory control strategies for hybrid electric vehicles. May 2007. IEEE, Transactions on control systems Technology.
- [9] L. Ljung T. Glad. *Reglerteori - Flervariabla och olinjara metoder*. Second Edition.
- [10] B. Egardt V. Larsson, L. Johannesson. Impact of trip length uncertainty on optimal discharging strategies for phev. June 2010. Advances in Automotive Control (IFAC).
- [11] L. Wang. *Model Predictive Control System Design and Implementation Using Matlab*.
- [12] J. Y. Wong. *Theory of Ground Vehicles*. Third Edition.

